SiC/SiC ceramic matrix composites with BN interphase produced by gas phase routes: An overview

Pierre Fenetaud, Sylvain Jacques

Open Ceramics 15 (2023) 100396

Contents lists available at ScienceDirect

Open Ceramics

journal homepage: www.sciencedirect.com/journal/open-ceramics

SiC/SiC ceramic matrix composites with BN interphase produced by gas phase routes: An overview

Pierre Fenetaud, Sylvain Jacques *

LCTS UMR 5801, CNRS - University of Bordeaux, 3 allée de la Boétie, 33600, Pessac, France

ARTICLE INFO

Handling Editor: Dr P Colombo

Keywords:
Ceramic matrix composite
Ceramic fibre
BN interphase
SiC/SiC composite
CVD/CVI
Mechanical behaviour
Oxidation/corrosion

ABSTRACT

The introduction of ceramic matrix composites (CMCs) into the hot sections of aircraft engines offers significant weight and fuel efficiency gains. The result of decades of research and development, CMCs are based on silicon carbide. They consist of a matrix reinforced with the latest generation of continuous fibres. The non-brittle behaviour of these materials is achieved by the "interphase", a thin coating of fibres. Boron nitride is the interphase material chosen to act as a mechanical fuse and to withstand the conditions of matrix manufacture and composite application. This paper considers the influence of the interphase on the mechanical properties of these CMCs and their behaviour in the different environments for which they are intended. Finally, the different preparation methods studied in the laboratory and the production methods used in industry are discussed, focusing on the gas phase routes.

1. Introduction

With the aim of reducing fuel consumption and pollutant emissions from aircraft engines [1], ceramic matrix thermostructural composites are of great interest. Indeed, these materials are paving the way for new, lighter engines that offer a more complete combustion thanks to their high operating temperatures. The resulting lightweighting of parts and the reduction of combustion by-products such as nitrogen oxides, made possible by the use of ceramic matrix composites (CMCs), are in line with these objectives.

Traditionally dedicated to military or aerospace applications, CMCs are engineered materials that are complex and expensive to produce. The potential of these new materials has been hampered by various technological barriers, which have been the focus of extensive work over the last few decades to make these materials more reliable, better understood and easier to manufacture. Process development has thus led to the introduction of these CMCs in civil aviation. They can be divided into two categories: oxide-based and non-oxide [2]. In the latter category, composites made of silicon carbide-based fibres and matrices (SiC/SiC) are intended for the manufacture of turbine parts for the hot sections of engines (blades, vanes, shrouds) [3,4]. In order to provide an interesting mechanical behaviour and the ability to be damaged without critical cracking, SiC/SiC contain a mechanical fuse. This particular component is in the form of a thin film coating the fibres, called the interphase. Historically, the interphase was made of pyrolytic carbon, but today it is more commonly made of pyrolytic boron nitride.

2. SiC/SiC composites

2.1. Background

Ceramics are inorganic, non-metallic materials that are generally divided into three categories: traditional ceramics (pottery, earthenware, stoneware, porcelain, etc.), glass or cement and, finally, technical ceramics (carbides, nitrides, aluminas, etc.) [5]. This last category has many industrial advantages: low density, high melting point, rigidity, mechanical resistance at high temperatures, chemical inertia and resistance to fatigue, creep and abrasion. Unlike plastically deformable materials such as metals, ceramics have the disadvantage of being brittle. This limits their use as structural materials.

A composite material is defined as a heterogeneous combination of several immiscible materials. It has a more interesting overall behaviour than its constituent materials taken separately. This concept was born out of the need to combine the advantages and/or to limit the disadvantages of certain materials. They are often used in applications where strength, lightness and reliability are required. There are many examples of natural composites, such as wood or bone, and man-made composites, such as concrete or glass fibre/epoxy composites. They consist of at least

* Corresponding author.
E-mail address: jacques@lcts.u-bordeaux.fr (S. Jacques).

https://doi.org/10.1016/j.oceram.2023.100396
Received 16 December 2022; Received in revised form 9 June 2023; Accepted 20 June 2023
Available online 20 June 2023

two different constituent materials, a reinforcement and a matrix. The reinforcement is usually in the form of particles or discontinuous (short) or continuous (long) fibres. It carries the mechanical load. The matrix surrounds the reinforcement. It provides cohesion and load transfer. It often has a protective function for the reinforcement (chemical attack, moisture, etc.).

In today's aircraft jet engines, the internal mechanical parts are exposed to a high-speed gas stream containing water vapour at high temperatures and pressures. This is the case, for example, with turbine blades and shrouds or combustor liners. These parts are typically made of nickel-based superalloys. These metallic materials offer a good compromise between mechanical strength, creep resistance and corrosion resistance at high temperatures, which is necessary for proper functioning in the environment in which these parts are located. However, these metallic materials are limited by maximum operating temperatures of around 1100 °C for densities of around 8. Current technological challenges are driving the aerospace industry to develop materials with excellent mechanical properties for higher operating temperatures. These new materials, known as thermostructural materials, have been the subject of research for more than half a century. Among the objectives that structure the development of these new materials, there are two main axes [6–9]:

- for equivalent properties, a reduction in weight induced by less dense materials,
- improved fuel efficiency through higher operating temperatures.

For this purpose, the expected properties of thermostructural materials include mechanical strength and creep resistance at high temperatures, oxidation resistance in corrosive atmospheres (air + water), reduced density compared to superalloys, and reliability allowing thousands of hours of operation without the risk of critical damage [7,10,11]. In this context, thermostructural composites, and more specifically CMCs, are being investigated and developed. CMCs are textured ceramic materials that combine a ceramic reinforcement, usually continuous fibres, with a ceramic matrix. Due to crack deflection phenomena, caused for example by a network of microporosities or specific interfacial layers, CMCs exhibit pseudo-ductile fracture behaviour. It is thus possible to obtain a non-brittle ceramic material [12–14]. By convention, CMCs are referred to as "reinforcement material/matrix material" (e.g. C/SiC for a carbon fibre reinforced silicon carbide matrix).

CMCs are used for parts exposed to extreme conditions. C/C composites can be found in spacecraft heat shields or in rocket nozzles [15,16]. However, their use in oxidising atmospheres is limited because, for example, they decompose into CO and CO_2 at 450 °C when in contact with air. In order to use CMCs in the Earth's atmosphere at higher temperatures and for longer periods, composites based on oxidation-resistant materials have been investigated. It is thus possible to replace carbon with oxides (mullite, alumina), nitrides (Si_3N_4) or carbides (SiC).

Oxide-based CMCs are insensitive to oxidation, but have poor mechanical properties at high temperatures and become brittle above 1000 °C, due to the sintering of the porous matrix. The application range of SiC/SiC composites is extended by better thermal conductivity and creep resistance at high temperatures. In addition, silicon carbide is a refractory material which is passivated in dry air at atmospheric pressure, forming a surface SiO_2 scale which generally protects it from oxidation. The appearance of the first long fibres based on silicon carbide [17] and the mastery of the infiltration process of the SiC matrix from methyltrichlorosilane [12,18] have made SiC/SiC composites the materials of choice for the manufacture and use of CMCs for aeronautical applications. Fig. 1 shows the specific strength of the different types of CMC as a function of the operating temperature and in comparison with metal alloys [8]. One of the reasons for the good ranking of these new materials is their density, which is two to three times lower

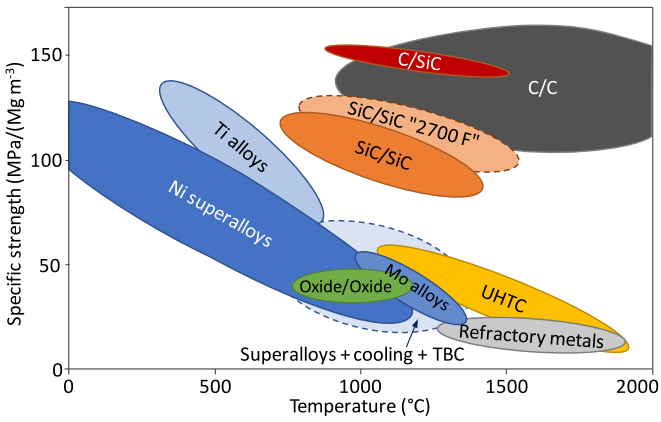

Fig. 1. Specific strength as a function of the temperature for various metals and CMCs - adapted from [8].

than, for example, superalloys. SiC/SiC composites are now an alternative to single crystal superalloys for structural parts with operating temperatures in excess of 1300 °C and lifetimes of several thousand hours [19]. CMC parts are now being used in the hot section of GE Aviation's commercial aircraft engines, which have been certified by European and US civil aviation safety authorities in 2016 and 2020 [9,20].

2.2. Silicon carbide

The only binary compound in the Si-C system is SiC [21], historically known as carborundum. The carbon and silicon atoms are organised in three crystal systems: cubic, hexagonal or rhombohedral. One of the peculiarities of SiC is its polytypism, with more than 150 polytypes ranging from cubic SiC-3C to numerous hexagonal (4H, 6H, etc.) and rhombohedral (15R, etc.) structures [22–24]. The carbon and silicon atoms form stacks of monoatomic layers in three possible atomic arrangements. These layers are commonly referred to as A, B and C. Thus 3C-SiC can be distinguished from 4H-SiC or 6H-SiC by their respective repeating sequences ABCABC, ABCBABCB and ABCACBABCACB (Fig. 2).

The Si-C bond is predominantly covalent (88%) based on the Pauling scale, with a distance of about 0.189 nm between the two atoms [26,27]. The importance of strong chemical bonds in SiC gives it properties similar to diamond. It has a high hardness of 9.5 on the Mohs scale (10 for diamond, 7 for quartz) with excellent chemical and thermal stability and high thermal conductivity. SiC remains solid up to about 2500 °C in an inert atmosphere before decomposing. It is passivated in air from 800 °C, forming a protective SiO_2 scale. SiC is resistant to chemical attack at room temperature by most known solutions (acids and bases), but it is attacked by molten salts such as KOH, NaOH or PbF_2 in the presence of oxygen [27,28]. Due to its excellent mechanical, chemical and refractory properties, SiC is used as an abrasive, as a shielding material or as a high temperature furnace lining. Table 1 lists some properties of SiC for the two most common polytypes, 3C-SiC and 6H-SiC. The form commonly found in SiC/SiC composites is similar to the cubic 3C-SiC form, also called β-SiC, including a greater or lesser amount of stacking faults.

2.3. SiC fibres

The first attempts to produce continuous SiC fibres date back to the 1960s when silicon carbide was deposited by the gas phase route on the surface of boron, tungsten or carbon filaments as a core [29,30]. Continuous SiC fibres synthesised on a tungsten core (Sigma from British Petroleum) or carbon core (SCS from Textron) are now commercially available with diameters greater than 100 μm.

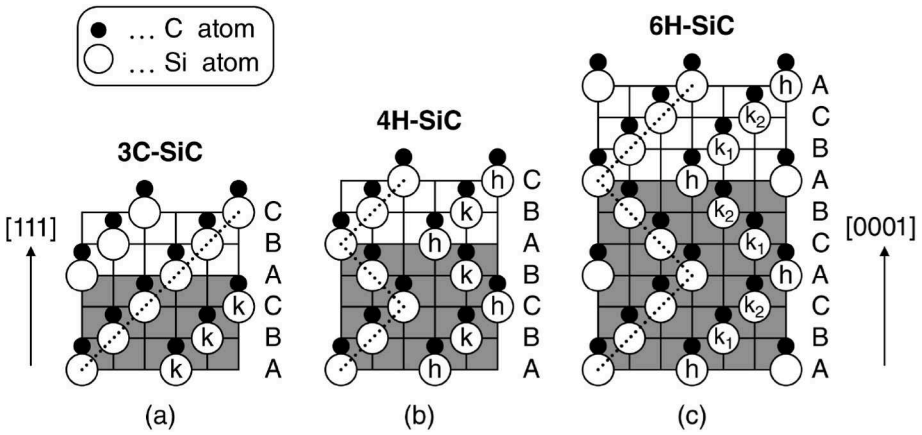

Fig. 2. Schematic structures of (a) 3C-SiC, (b) 4H-SiC, and (c) 6H-SiC [25].

Table 1
Properties of 3C-SiC and 6H-SiC at room temperature [25,27].

Properties	
Density ($g{\cdot}cm^{-3}$)	3.21
Lattice constants (nm)	$a = 0.436$ (3C) $a = 0.308/c = 1.512$ (6H)
Young's modulus (GPa)	450
Poisson's ratio	0.2
Thermal conductivity ($W{\cdot}cm^{-1}{\cdot}K^{-1}$)	3.2 (3C)/3.6 (6H)
Emissivity vis-IR (300K-1400K)	>0.90
Refractive index in the visible range	2.6 - 2.8

The work initiated by Yajima et al. on polycarbosilanes has led to the development of continuous silicon carbide-based fibres with a fine diameter (around 10 μm), which makes them flexible [17,31–33].The SiC and Si-C-O fibres produced by various manufacturers (COI Ceramics, Dow Corning, Nippon Carbon, Ube Industries, etc.) differ in the preceramic polymer chosen and in the manufacturing process. The main polymers used are polycarbosilanes (PCS), polyaluminocarbosilanes (PACS) and polytitanocarbosilanes (PTC). Fibres are generally in the form of multifilament tow on spools, typically consisting of 500–3000 individual filaments. Three generations of fibres can be distinguished, reflecting production processes that are increasingly favourable to crystallised fibres of near-stoichiometric composition [34,35]. The changes in fibre microstructure are shown in Fig. 3.

The main reinforcement used in SiC/SiC composites with BN interphase for aerospace applications consists of continuous SiC fibres, mainly third generation fibres [36]. These are in particular Hi-NicalonTM type S (HNS) fibres produced by NGS Advanced Fibers Co., Ltd., a joint venture corporation between Nippon Carbon (Japan), Safran (France) and GE Aviation (USA). Today, they are the only SiC-based fibres used as reinforcement in CMC parts of certified commercial aircraft engines [9]. The production of these fibres is characterised by electron beam curing to avoid the introduction of oxygen and thus the amorphous Si-O-C phase, followed by a pyrolysis step under H_2 before the final pyrolysis under Ar at very high temperature to reduce the presence of free carbon [37]. As a result, these third-generation fibres have a near-stoichiometric composition with a C/Si molar ratio of 1.05 and a residual oxygen content of 0.2 wt %. They retain their mechanical strength up to temperatures of around 1600 °C in an inert atmosphere [38,39]. Above this temperature, traces of oxygen produce gaseous species that cause porosity and flaws of submicron size. These

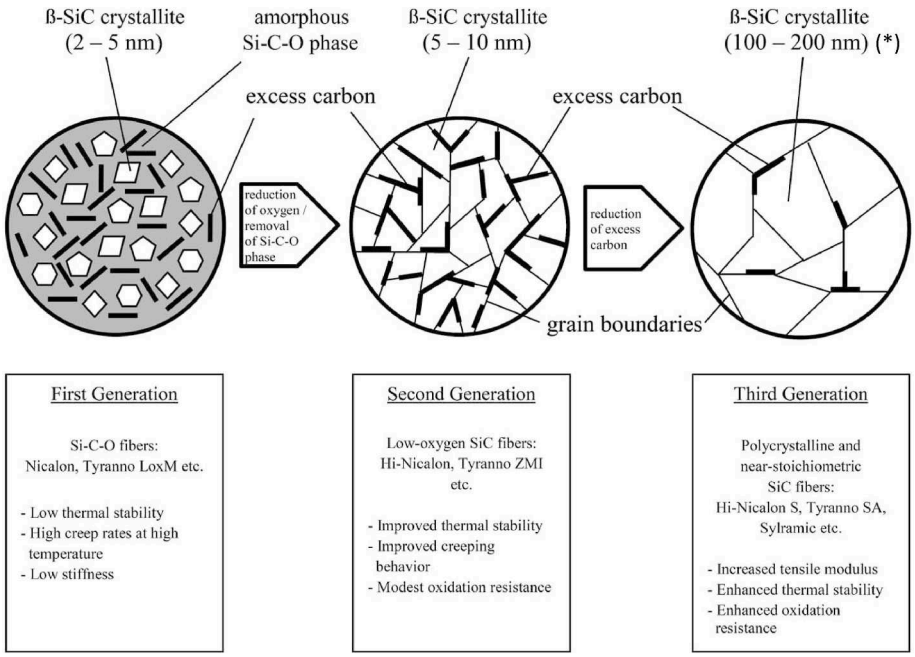

Fig. 3. Differences between the three generations of commercially available SiC-based fibres [35] (* 50–100 nm according to Ref. [34]).

reduce the macroscale mechanical strength. HNS fibres have excellent oxidation and creep resistance up to 1200 °C [39–41], exceeding that of previous generations [42,43]. Their Young's modulus is also higher, but their mechanical strength at room temperature and at high temperatures remains dependent on the residual oxygen content [44]. They therefore offer favourable behaviour for thermostructural applications while maintaining properties close to those of monolithic SiC [41,45–47]. HNS fibres are mainly composed of β-SiC (3C) with 111 stacking faults, resulting in a low presence of the hexagonal phase in X-ray diffraction analysis [48]. The presence of a small amount of free carbon in a turbostratic form limits the growth of silicon carbide grains during the manufacturing process. This would explain why these fibres retain good mechanical strength after exposure to high temperatures. The good purity of the HNS fibres also explains their improved creep resistance compared to competing fibres with larger grain sizes but containing unfavourable sintering aids [49]. They can have a carbon-rich surface layer approximately 80 nm thick [48]. As a result, the as-received HNS fibre has a specific resistivity of 2.9 Ω cm. This increases to 200 Ω cm when the surface layer of the fibre is removed [44].

An HNS tow consists of approximately 500 individual fibres. After processing, a polyvinyl alcohol (PVA) sizing is applied to the tow to facilitate winding, handling and weaving. The properties of HNS fibres are compared to other 3rd generation SiC-based fibres in Table 2.

Fibres can be incorporated into CMCs in the form of 1D fibre reinforcements (e.g. straight tows), 2D fibre reinforcements (e.g. stacking of woven plies) or even 3D fibre structures (e.g. with interlock tows to limit delamination between the plies). For this purpose, the continuous fibres can be woven into the shape of the final part to give a preform. Weaving techniques have evolved according to the type of mechanical loading and the complexity of the parts to control the anisotropy of the "skeleton" that makes up the 3D preform [52,53].

3. SiC matrix synthesis processes

The manufacture of SiC/SiC composites is a complex and costly multi-step process [11,41,54]. The matrix processing route, also known as the CMC densification stage, is a critical step. The different ranges of industrial SiC/SiC composites are regularly differentiated by the densification route chosen, as it has a significant impact on the final properties is significant. Densification can only be achieved through sophisticated processes that require certain compromises in terms of final quality and manufacturing cost.

Table 2
Details of the manufacture, elemental composition and properties of the 3rd generation of SiC-based fibres [34,41,47,48,50,51].

Trade mark	Tyranno SA (1 and 3)	Sylramic	(Super) Sylramic-iBN	Hi-Nicalon type S
Manufacturer	Ube Ind.	Dow Corning/COI Ceramics	COI Ceramics	NGS
Precursor	PACS	PTC + B	PTC + B + N_2	PCS
Cross linking method	Oxygen	Oxygen	Oxygen	Electron irradiation
Si (wt. %)	68	67	65	69
C (wt. %)	31	28	28	31
O (wt. %)	0.3	0.9	0.3	0.2
Impurities (wt. %)	Al (1)	B(2) N(<1) Ti (2)	B(2) N(2) Ti (2)	/
Average diameter (μm)	7.5–11	10	10	12–13
Fibres/tow	800–1600	800	800	500
Density ($g{\cdot}cm^{-3}$)	3.02	3.05	3.05	3.05
Young's modulus (GPa)	375	400	400	420
strength (GPa)	2.8	3.2	3.0–3.1	2.6-2.8
Fracture strain (%)	0.7-0.9	0.8		0.6
Grain size (nm)	200	100	>100	50–100

3.1. Slurry cast and ceramic route

A densification route derived from conventional ceramic routes uses slurry cast impregnation. A suspension of particles in a solvent, often aqueous and sometimes accompanied by dispersants, flocculants, binders, wetting agents and/or sintering additives, is introduced into the fibre preform. Sintering can then take place, usually in a controlled atmosphere and under high pressure. Very high temperatures (>1600 °C) and high pressures are required to sinter pure silicon carbide [55,56]. This is a significant barrier to the use of sintering for to produce the matrix. High-pressure processes, assisted by sintering additives such as Al_2O_3, Y_2O_3 or SiO_2, allow a reduction in sintering temperature and an increase in matrix density [56–58]. This ceramic route is therefore limited to the production of composites reinforced with unidirectionally oriented SiC fibres; it has also been used for Si_3N_4 matrices [59]. Rapid sintering methods such as spark plasma sintering are being developed to sinter SiC and limit fibre degradation [60]. Mechanical stresses resulting from the pressure applied during sintering are also a barrier to the use of this technique with 3D fibre preforms. The slurry cast method is often combined with other densification methods, such as polymer impregnation and pyrolysis [61–63] or melt infiltration [54,64,65], which are described below. This combination limits the pressure and temperature required to densify the ceramic, while the powder allows the SiC content of the matrix to be increased (less free silicon or free carbon).

3.2. Polymer impregnation and pyrolysis

The polymer impregnation and pyrolysis (PIP) process can be carried out with polycarbosilanes (PCS), for example. The air-sensitive preceramic polymer is then cross-linked and pyrolysed in an inert atmosphere. The conversion to ceramic is accompanied by volume shrinkage. To increase the density of the CMC, it is necessary to perform several consecutive PIP cycles [66]. However, due to the difficulty of penetrating the polymer into the small closed pores present in the converted SiC matrix, the minimum final porosity is typically around 5%. This low-yield process hardly results in high-purity matrices. Indeed, matrices contain impurities such as oxygen and free carbon. In addition, the matrices obtained are poorly homogeneous and often cracked due to shrinkage [67].

3.3. Melt infiltration and reactive melt infiltration

Melt infiltration (MI) densification is now a common process for producing dense matrices. It is used as a complement to other methods that have already allowed partial densification of the fibrous preform with carbon or silicon carbide. The porous network provides sufficient capillary pressure to lead to infiltrate liquid silicon throughout the composite [54,68,69]. The final part is almost completely densified, with very low residual porosity (less than 5%) for shorter densification times than with the other routes. However, the presence of free silicon in the matrix is detrimental to the temperature and creep resistance of the composite [70]. In addition, silicon is very reactive towards the constituents of the CMC, such as fibres or possible interfacial layers. It is therefore necessary to protect these constituents prior to the MI step. For this purpose, a layer of SiC or Si_3N_4 is usually deposited beforehand [54,71]. The use of a SiB_x alloy appears to be less chemically aggressive to preform constituents than pure silicon [72–74]. The addition of free carbon, in the form of filler, fibre surface layer or pre-densification, subsequently allows the formation of SiC by reaction with liquid silicon. This is known as reactive melt infiltration (RMI). The simple

addition of a thin surface layer of carbon in addition to the fibre coatings improves the adhesion between the matrix and the preform [75].

The MI process is carried out at temperatures above the melting point of silicon, 1414 °C, and in an inert atmosphere or vacuum. In the case of RMI, the reaction between the components is exothermic, which further increases the temperature locally [76,77]. The fibre reinforcement must withstand these temperatures, so only second and third generation SiC fibres are used. The capillary pressure required to fill the pores is strongly dependent on, among other things, the wettability of the materials by liquid silicon. For example, SiC has an excellent wettability with a wetting angle ranging from 8 to 40° depending on the work, in contrast to SiO_2 which has wetting angles of 85–90° [78–81]. However, the wetting angle on SiC increases with SiB_x alloys. Si_3N_4 gives wetting angles of 40°–90° depending on the surface condition, quality and measurement method [78–81]. Its wettability by Si appears to be improved by the presence of boron and by high temperatures [78].

3.4. The gaseous route

A common route for densifying the SiC matrix in CMCs is chemical vapour infiltration (CVI), which is derived from chemical vapour deposition (CVD) [82].

3.4.1. Principle of the CVD process

This section is mainly based on the literature by Besmann et al. [83], Golecki [84], Belmonte [85], Carlsson and Martin [86] and Frey [87].

Chemical vapour deposition (CVD) is a process for the production of thin solid films from gaseous precursors and an energy source. Its origins date back to 1880 with patents by Sawyer and Man on the deposition and densification of carbon filaments for the manufacture of lamps [88,89]. It was developed industrially in the mid-twentieth century for the deposition of carbide and titanium nitride coatings on cutting tools [90]. CVD involves chemical reactions at the surface of the substrate. There are several variants of CVD that can be distinguished by the deposition conditions, the type of precursors used or the activation source employed. In all cases, however, the process involves a series of sequential steps as shown in Fig. 4:

1 Convective transport and diffusion of the reactive species in the gas mixture,
2 Adsorption of the reactive species onto the substrate surface,
3 Surface diffusion of the reactive species, heterogeneous reaction(s) leading to formation of clusters and by-products and the germination and/or crystal growth of the deposit,
4 Desorption of gaseous reaction by-products,
5 Diffusion and convective transport of by-products in the gas phase.

The reaction(s) in step 3 require(s) an activation energy, usually obtained by heating the substrate (radiative, laser etc.) or by high energy radiation (UV, etc.). A sufficiently high substrate temperature promotes surface diffusion and results in homogeneous film growth.

Under certain conditions, two stages, 0 and 6, may occur before the diffusion and adsorption of reactive species on the surface and after the desorption and diffusion of by-products, respectively. Chemical reactions between the initial precursors can occur in the gas phase. Species that are not stable under ordinary conditions of pressure and temperature (intermediates or effective precursors) are then likely to appear. These gas phase maturation phenomena are grouped under the term "homogeneous reactions", as opposed to heterogeneous reactions that occur at the surface of the substrate. Gas phase maturation depends on the nature of the reactive mixture, the reactor design and the deposition conditions. In particular, it is enhanced at high pressure, high temperature, low gas velocity, large reaction volume or low dilution of the reactants in the carrier gas.

The types of chemical reactions that give rise to CVD coatings typically include:

- thermal decomposition, or pyrolytic reactions,
- nitridation and carburisation,
- reduction reactions, mainly with H_2,
- oxidation reactions (with O_2, CO, CO_2, N_2O etc.),
- dismutation reactions,
- exchange reactions,
- coupled reactions.

Under extreme operating conditions (very high temperatures and pressures), the chemical reaction kinetics are sufficiently high to lead to the formation of solid products in the gas phase, despite the absence of a solid substrate. The formation of soot or powder in the reaction zone is then observed. This phenomenon, known as homogeneous phase nucleation, is detrimental to achieving a coating and should be avoided.

3.4.2. Process parameters and deposition regimes

In conventional thermal CVD, the deposition conditions used, such as pressure, temperature or mass flow rates, have a strong influence on the growth rate of the coating. This is because these parameters preferentially affect certain steps of the CVD process. Depending on the limiting step(s), several deposition regimes can be distinguished. The three main regimes, described in more detail below, are shown in the Arrhenius plot in Fig. 5a.

Chemical reaction-limited regime (CRR): This corresponds to the regions of low temperature, low pressure and high dilution of the reactant(s). Heterogeneous reaction step 3 is the rate-limiting step. The

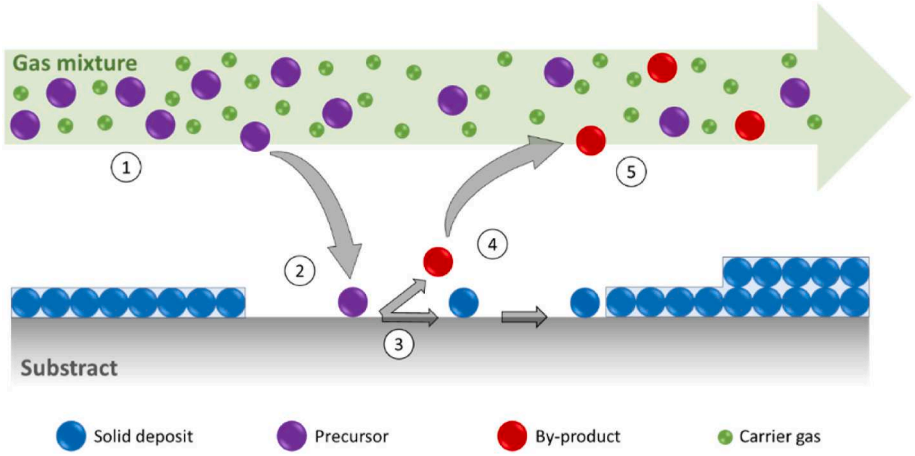

Fig. 4. Principle and steps of CVD.

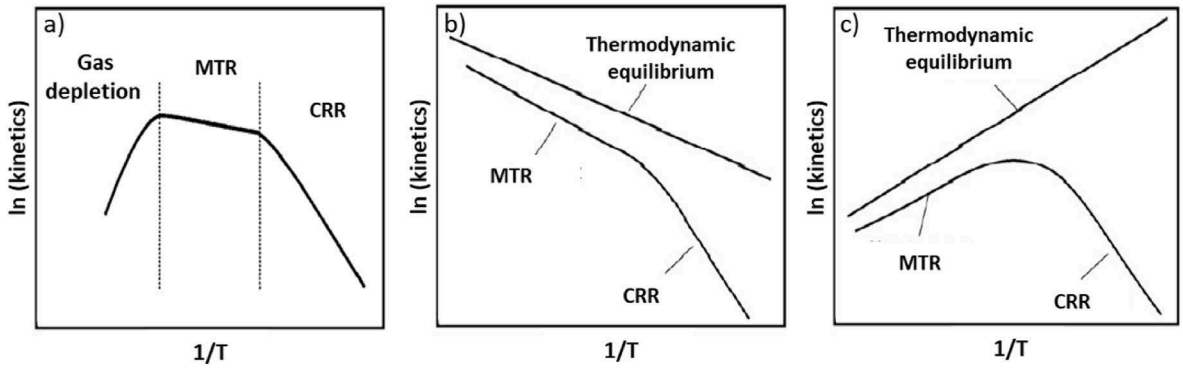

Fig. 5. Schematic Arrhenius plots showing the temperature dependence of the deposition rate and the different regimes in CVD (a) [84]. Transition between CRR and MTR for endothermic (b) and exothermic (c) processes [86].

reaction kinetics are thermally activated, with the evolution of the coating growth rate being strongly dependent on the substrate temperature. The other parameters have little influence on the growth rate. The CRR is therefore characterised by a linear dependence of the logarithm of the growth rate on the reciprocal of the temperature, according to an Arrhenius law [91,92]. The slope of the Arrhenius curve observed in the CRR (Fig. 5a) corresponds to the activation energy of the reaction divided by the ideal gas constant. The activation energy of a CVD coating in the CRR is generally in the range of 100–300 kJ/mol. Coating formation can also be limited by homogeneous reactions (step 0), where the growth rate depends on the temperature of the gas phase. This type of mechanism involves one or more effective intermediate precursors.

The mass transfer-limited regime (MTR): When the reaction kinetics are sufficiently high, for example at high temperatures, steps 1 and 2 as well as 4 and 5 become rate-limiting. Under these conditions, the ability of the system to promote diffusion and rapid adsorption and desorption of species determines the deposition growth rate. The process parameters that control diffusion, such as pressure or flow rates of gaseous species, become dominant in controlling growth rates. In contrast, the growth rate of the coating is only slightly dependent on the substrate temperature. A plateau of kinetics is observed in the Arrhenius curves, slightly increasing or decreasing depending on the type of chemical reaction involved (Fig. 5b&c).

Gas depletion: At very high temperatures, nucleation in the homogeneous phase leads to a decrease in the precursor concentration, which limits the growth rate on the substrate surface. Gas depletion is exacerbated by the reaction of the precursors on the hot reactor surfaces upstream of the zone of interest (reactor walls, sample holder, etc.). This phenomenon is detrimental to achieving a dense and homogeneous coating.

3.4.3. *Deposition in fibre preforms: the CVI batch process*

The term chemical vapour infiltration or CVI is used when a coating is formed by a CVD process in a porous substrate. The diffusion of the gas through the porous network into the core of the substrate becomes an essential additional step in the control of the CVI process. Indeed, the diffusion of the gas phase into the preform induces a depletion of the precursor proportional to the infiltration depth [83,93]. To overcome this issue and to promote uniform infiltration of the solid deposit into the pores, it is necessary to operate in CRR. Furthermore, gas infiltration is favoured at low pressure (1–100 mbar).

Densification of the SiC matrix in fibre preforms by CVI is widely used [2,3,82,94]. Its main advantages are very high purity, control of the crystallinity of the synthesised materials and the ability to infiltrate complex shapes without degrading the preforms. However, this process is time consuming, expensive and results in an imperfectly densified material. Indeed, an external sealing coating inevitably forms on the surface of the preform, eventually preventing the passage of precursor gases. The resulting residual porosity of around 15–20% is detrimental to the final properties of the CMC by limiting the thermal conductivity and mechanical strength of the matrix. In addition, the gases used and the reaction by-products are very often aggressive and/or toxic (halogenated gases).

Among the different technologies, two main operating principles can be distinguished, depending on the heating method used.

In hot wall reactors under isothermal-isobaric CVI (I-CVI) conditions, the entire reactor chamber is heated. The precursor gases therefore react with the substrates as well as the walls, forming a solid deposit on all hot surfaces. The homogeneous temperature of the gas mixture facilitates control of the deposition process and gas flow, but results in higher precursor consumption. This type of reactor is widely used in industrial mass production of CMCs [95]. They provide significant gas maturation and are often necessary to achieve the desired SiC matrix quality. Deposition temperatures must be limited, typically around 1000 °C, to ensure CCR and infiltration quality. This has a negative effect on growth rates and requires long densification cycles of up to several hundred hours. Because of the deposition times and the high cost of the equipment (vacuum chambers, pumps, gas lines, etc.), industrial reactors are designed to process many parts simultaneously in systems of several metres in size (batch processing CVI). An example of a CVI facility is shown in Fig. 6.

In cold wall reactors, only the substrates are heated, limiting homogeneous reactions and reactant consumption. Such reactors also allow higher deposition temperatures without homogeneous phase nucleation. Deposition kinetics are therefore potentially higher. This reactor design requires direct heating of the preform, depending on the material, or a local heating source. For substrates containing carbon, inductive or resistive heating can be used. Microwave absorption also allows the heating of the substrate via direct, indirect or hybrid (susceptor + substrate) coupling [98,99]. Alternatively, guided heat sources such as mirrors and/or focusing devices (halogen lamps, arc-imaging furnace etc.) or laser sources can be used. These technologies allow the heating of a wide range of materials, but create large temperature gradients in both the substrate and the reactor. In the reactor, these thermal gradients are mainly caused by radiative exchange between the cold walls and the hot substrate, as well as convective losses. They cause convection currents that disturb the gas flow. The result can be non-uniform thickness, composition and morphology of the coating [83]. Within the substrates themselves, such as fibrous preforms, these gradients can be exploited in so-called thermal-gradient CVI processes to limit the seal coating and promote infiltration [84,94].

3.5. *Industrially manufactured SiC/SiC composites*

Various types of SiC/SiC composites have been developed, such as CMCs with a fully I-CVI-synthesised, self-healing matrix [100]. Currently, industrially developed SiC/SiC composites for aircraft engine hot sections are made with CVI-MI matrices. They therefore have a lower

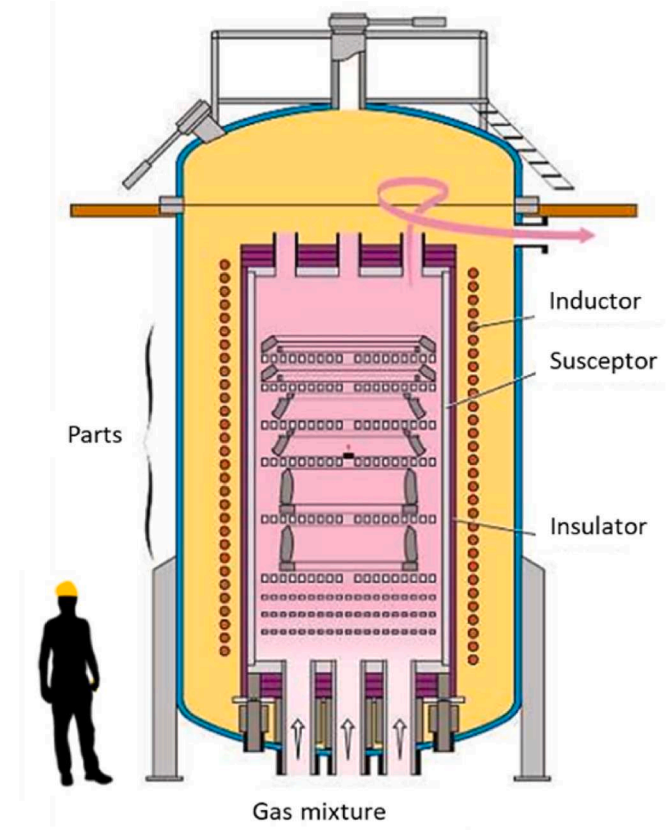

Fig. 6. Schematic representation and photograph of the top of industrial facilities for batch processing CVI [96,97].

porosity than full CVI matrix composites. State-of-the-art CMCs are most commonly produced in the following steps, with some variations depending on the manufacturer and the exact type of part that is required [3,6,41,54]:

- preform weaving (2D or 3D) of SiC tows and fibre desizing,
- deposition of one or more interfacial functionalisation and protective layers by CVD/CVI on all the fibres of the preform,
- introduction of SiC powders into the residual porosity e.g. by slurry cast method,
- densification by liquid silicon infiltration (MI),
- deposition of a silicon-based layer acting as a bond coat,
- deposition of an environmental barrier coating (EBC) as a top-coat.

The role of EBCs is to protect CMCs in service conditions from water corrosion and attack by calcium-magnesium alumino-silicate (CMAS) melts from dust, sand or ash. EBCs are most commonly deposited by air plasma spraying [101].

In a variant of CMC manufacture called "prepreg MI", the fibre protective layers and the matrix slurry are applied in a continuous process onto a moving fibre tow prior to forming the preform [68,102].

4. Interphase in SiC/SiC composites

4.1. Role of the interphase

Like any ceramic material, each component of a SiC/SiC composite is stiff and brittle. However, by controlling the behaviour of the fibre/matrix interfaces, a tolerance to mechanical damage can be achieved [103,104]. During loading, cracks propagating in mode I in the matrix are deflected in mode II along the fibres at the fibre/matrix interface instead of causing fibre failure. The composite thus exhibits a pseudo-ductile mechanical behaviour, allowing it to withstand impact or deformation without critical failure.

This toughness is achieved by introducing a preferential damage zone in the form of a thin layer or interface coating (less than 1 μm thick), referred to as the "interphase", between the fibres and the matrix [13,105,106]. The interphase must therefore be mechanically weaker than the matrix to act as a "mechanical fuse", i.e. to deflect matrix microcracks and protect the fibres from early failure. This avoids the brittle behaviour observed when the bond between the fibre and the matrix is too strong (Fig. 7a). Conversely, if the bond between the fibre and the matrix is too weak, the load levels carried by the CMC are reduced (Fig. 7b). In practice, the interphase allows the CMC to have an intermediate behaviour between the two extreme cases. The ideal case is the interphase that maintains a "rather strong" fibre-matrix bonding (Fig. 7c), resulting in a pseudo-ductile behaviour with a higher mechanical strength than the case of a "rather weak" fibre-matrix bonding (Fig. 7d) [107]. The strength of this bond can be directly measured locally using micromechanical single-fibre push-out tests, which provide the interfacial shear stress (ISS) [108–110]. Finally, the interphase must be compatible with the constituent materials of the CMC, adhesive and able to withstand high operating temperatures. CMCs with an interphase are tough and can have a higher maximum strain and stress than the brittle matrix alone.

The mechanical behaviour of a SiC/SiC composite is determined by

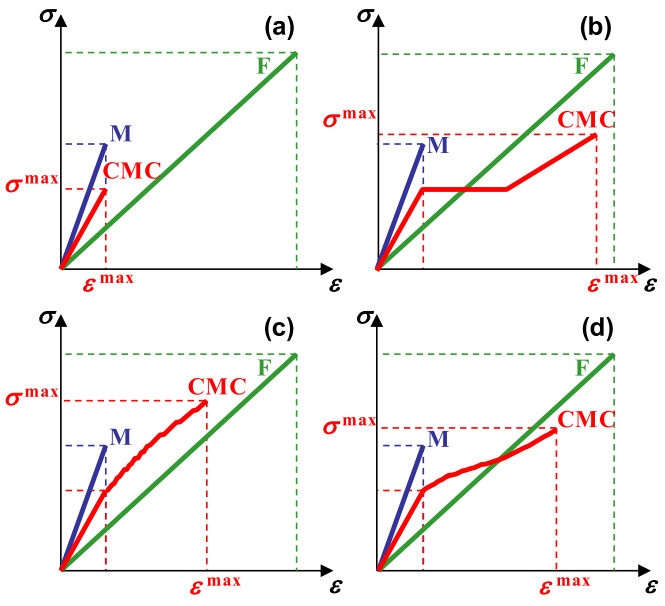

Fig. 7. Schematic stress-strain curves for SiC fibres (F), monolithic SiC matrix (M) and SiC/SiC composite (CMC) with too strong (a), too weak (b), rather strong (c) and rather weak (d) fibre-matrix bonding.

the fibre-interphase-matrix system, which in turn depends on the failure mechanisms at the interfaces. Several types of materials have been studied to form the interphase:

- porous films,
- lamellar and anisotropic graphite-like materials.

Multilayer coatings are also interesting solutions, by forming an interfacial system combining a crack-deflecting material with a lamellar or layered crystal structure and layers of more oxidation-resistant, and glass-forming material, such as SiC or $B_{13}C_2$ for example [106,111–113].

4.2. Interphase materials

4.2.1. Porous materials

The use of a porous matrix is common in oxide composites (alumina, mullite, etc.) to accommodate stresses and allow crack deflection according to the "weak matrix" approach [114,115]. The introduction of porous interphases is also mentioned, although not very common [116]. There are few reports of such interphases in SiC/SiC composites. The work of Verdenelli et al. showed the possibility of depositing a porous layer consisting of a mixture of Al_2O_3 and SiO_2 on SiC fibres by sol-gel dip-coating. The authors demonstrated that the coated fibres retain their properties after treatment in air at 1200 °C [117]. However, model composites with these interphases exhibit brittle behaviour [118]. The potential of porous interphases for SiC/SiC composites remains limited to date. This is partly due to the risk of sintering when used at high temperatures, which can lead to catastrophic degradation of their crack deflection capability. Furthermore, porous TiC layers [119] and multilayer coatings of porous TiC and SiC [120] do not appear to provide sufficient deflection to avoid brittle fracture.

4.2.2. Lamellar materials

The materials with a lamellar structure used in CMC interphases consist of a stack of atomic planes, similar to graphene, characterised by a more or less pronounced structural anisotropy. The presence of weak inter-plane bonds (van der Waals interactions) favours crack deviation. Pyrolytic carbon, or PyC, and pyrolytic boron nitride, or pBN, are the main representatives.

Applications envisaged for CMCs include high temperatures in oxidising and corrosive atmospheres. Under service conditions, microcracks formed within SiC/SiC provide pathways for the external atmosphere, including O_2 and H_2O. PyC oxidises from 450 °C in the presence of an oxygen-containing atmosphere to form gaseous CO_2 and CO. During oxidation, pBN forms liquid B_2O_3 which slows down the oxidation process. BN interphases can resist active oxidation up to temperatures of about 900 °C, depending on the degree of crystallisation and orientation of the basal planes [121–123]. Nevertheless, B_2O_3 evaporates in the presence of water in the form of $H_xB_yO_z$ species. Furthermore, pBN is not very stable in the presence of water at room temperature and hydrolyses to form hydrated ammonium borates [124,125]. Compared to the matrix and the SiC fibres, the interphase is the weak component of the CMC from both a mechanical (beneficial) and chemical (detrimental) point of view. During the MI step, the interphase may come into contact with liquid silicon. PyC is then rapidly consumed to form SiC. Conversely, BN is poorly wetted by Si (wetting angle ≈ 145°) and has a higher resistance to its chemical attack [79,80]. Boron nitride has therefore become the interphase material of choice for SiC/SiC composites for the next generation of aircraft engines. It offers a very good compromise between crack deflection in these composites and oxidation/corrosion resistance. The recent paper by Chen et al. provides a comprehensive and complementary review of BN interphases for SiC/SiC composites [126].

4.2.3. Boron nitride

BN is the only solid binary compound in the B-N system [127,128]. Depending on the conditions under which it is produced, boron nitride exists in several crystalline structures, as shown in Fig. 8. A distinction should be made between sp^2-hybridised BN forms (sp^2-BN) with a hexagonal or rhombohedral structure (h-BN and r-BN), and sp^3-hybridised BN forms (sp^3-BN) with a cubic or wurtzite structure (c-BN and w-BN). The sp^3-hybridised forms, referred to as "hard phases", are industrially synthesised mainly under high-pressure and high-temperature conditions [128,129]. These hard phases are not suitable for this application and will not be discussed in detail here.

The sp^2-BN have an "ordered" structure of parallel atomic planes. These basal planes consist of B_3N_3 hexagons. A distinction is made between hexagonal BN, h-BN, with an ABAB... type stacking sequence, and rhombohedral BN, r-BN, with an ABCABC... type stacking sequence [130,131]. Some works also mention other polytypes such as 12R-BN or 24R-BN [132]. These sp^2-BN structures result in a pronounced structural anisotropy, corresponding to the presence of strong intra-plane covalent bonds and weak inter-plane bonding forces as in graphite. The semi-opaque, white appearance of h-BN has earned it the name "white graphite". It is used as a lubricant, electrical insulator and thermal conductor. It is also used as a crucible or protective material because it is chemically inert and is not wetted by most liquid metals and non-metals. It can withstand temperatures of 1400 °C in a vacuum and over 2800 °C in an inert atmosphere [128].

Similar to PyC, a turbostratic structure of sp^2-BN, termed t-BN, is

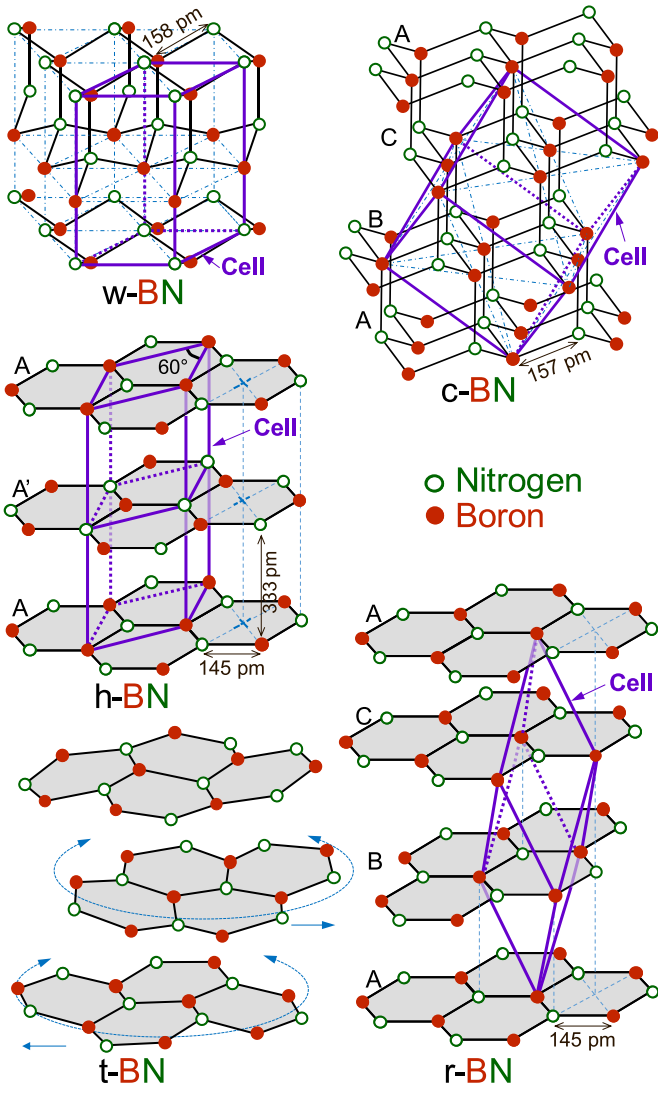

Fig. 8. Crystal structures of BN - adapted from [128,134].

found in pBN, which is less ordered than h-BN or r-BN. It is characterised by local stacking defects such as rotations, translations and curvatures of the atomic layers, which include interplanar covalent bonds. These defects increase the strength of the interplanar bonds compared to a perfectly ordered lamellar structure such as h-BN. A t-BN interphase can therefore allow a rather strong fibre-matrix interfacial bonding, which is favourable for the mechanical behaviour of CMCs, provided that a cohesive failure is achieved in the BN coating. t-BN is usually synthesised by CVD at lower temperatures and/or higher pressures than h-BN and r-BN [133].

It is common to observe an amorphous and isotropic structure for BN obtained at low temperature, generally referred to as a-BN. Many papers mention the synthesis of very weakly crystallised isotropic BN [135–138]. The optical and dielectric properties of these materials are exploited for microelectronic applications. In gaseous route processes, the degree of crystallisation of BN as well as its structural anisotropy increases with the deposition temperature [125,133,135,139]. The synthesis of BN interphases by CVI in fibrous preforms is generally limited to temperatures below 1000 °C and is carried out at low pressures (100–1333 Pa) [140–142]. It results in t-BN or even a-BN, with the occasional appearance of r-BN coherence domains if the interphase deposition temperature could be increased [143]. The properties of the main allotropes are given in Table 3.

4.3. Fibre-matrix bonding and mechanical behaviour of SiC/BN/SiC composites

Works on the effect of the thickness and microstructural organisation of BN interphases on the fibre-matrix bonds and the mechanical properties of CMCs have been carried out with the first generations of SiC fibres, namely Nicalon [150] and Hi-Nicalon [151,152]. While significant effects have been highlighted, the thermal instability of the fibres, sizing residues or unexpected phenomena during thermochemical treatments leading to the formation of voids/pores and/or undesired phases (free carbon and silica) at the interfaces tend to weaken the interfacial bonds. In the case of the latest generation of fibres, Morscher et al. observe debonding either at the fibre-BN interface (adhesive debonding or "inside debonding") or at the BN-matrix interface ("outside debonding") as a consequence of the local presence of carbon depending on the processing conditions [153]. ISS values measured by fibre push-out tests remain below 100 MPa. Rebillat et al. have shown that the bond between Nicalon fibres and BN interphases can be strengthened (resulting in ISS values in excess of 100 MPa) if the fibres have previously undergone a specific surface treatment [154]. In this case, crack deflection was only observed only in the BN interphase when it consisted of two sub-layers with a sufficiently weak interface between them. To achieve this, the second sublayer was synthesised under aggressive conditions and was highly crystallised. Similar observations were reported by Jacques et al. using Hi-Nicalon fibres and simplified 1D model composites [155]. Interesting results were also obtained by Jacques et al. using a non-aggressive precursor not commonly used in the industrial production of BN interphases and a deposition temperature of 1100 °C [156]. It has been shown that in some cases, BN interphases classically synthesised by CVI at relatively low temperatures (<1000 °C) and therefore poorly crystallised, were poor mechanical fuses and resulted in too strong fibre-matrix bonding. However, it is difficult to attribute this behaviour to the poor crystallisation degree of BN, or rather to its high sensitivity to air moisture if not stabilised by a post-infiltration heat treatment at well above 1000 °C [142]. These various difficulties, i.e. interference at the interfaces and the instability of BN with respect to ambient moisture in composites prepared under near-industrial conditions, have often prevented a clear conclusion on the influence of the BN interphase itself on the mechanical properties of the CMC, or even on the ability of the BN material itself to act as a mechanical fuse.

Table 3
Properties of a-BN, h-BN and c-BN at room temperature [128,144–149].

Form	a-BN	h-BN	c-BN
Space group	/	$P6_3/mmc$	$F\bar{4}3$ m
Lattice constants (nm)		$a = 0.2504$ $c = 0.666$	$a = 0.361$- 0.367
Density ($g{\cdot}cm^{-3}$)	2.03	2.1–2.3	3.45-3.49
Hardness (GPa)	10 (Knoop)	1.5 (Vickers)	40-80 (Knoop)
Young's modulus (GPa) (polyscrystalline)	/	120-200 (simulation)	800–900
Thermal conductivity ($W{\cdot}m^{-1}{\cdot}K^{-1}$)	3	63 (a/b) 1 (c)	1300

De Meyere et al. have shown that the thickness of the BN interphase influences the interfacial properties measured by push-out tests performed on third generation fibres in composites supplied by an industrial company [157]. However, the ISS values obtained with HNS fibres remain relatively low (~10–30 MPa depending on the interphase thickness and the position of the HNS fibre in the composite). Delpouve et al. were able to relate micro- and macro-mechanical properties to the thickness and crystallisation degree of BN interphases using single-ply model SiC/BN/SiC-Si composites reinforced with surface-treated HNS fibres (Fig. 9a&b) [158]. These composites are very representative of industrial composites designed for aero-engines and produced by CVI with conventional precursors and by MI. The interphase failure is cohesive, with matrix crack deflections occurring in BN, more or less close to the interface with the fibre. This study demonstrates that the BN material is definitely capable of acting as a mechanical fuse by itself (Fig. 9c). The low degree of crystallisation and anisotropy of a BN interphase synthesised by CVI at 900 °C results in a stronger fibre-matrix bond (ISS >100 MPa) and better CMC tensile and flexural mechanical properties than a high degree of crystallisation and anisotropy of an interphase synthesised at 1200 °C (ISS <50 MPa). For an interphase synthesised at 900 °C, a thickness of ~500 nm ("*9/T*") is preferable to a thickness of ~200 nm ("*9/t*").

5. SiC or Si_3N_4 as a protective layer for the interphase

The BN interphase coating, especially if synthesised by CVI at low temperature, must be protected from contact with air prior to matrix densification. Furthermore, liquid silicon is very corrosive with respect to the interphase and the fibres [70,73]. For example, it reacts with free carbon in the fibres, in addition to modifying the microstructure through catalysed recrystallization. Although liquid silicon hardly wets BN, it is still capable of degrading the interphase layer by forming, among others, Si_3N_4 [54,72,79,80].

For these reasons, a thin protective layer is deposited by CVD/CVI immediately after the deposition of the BN interphase. Several materials are relevant for this application. SiC is of obvious interest as it is identical to the matrix and close to the properties of HNS fibres. If its microstructure and purity are properly controlled, which is possible with gaseous route synthesis, SiC is capable of forming an effective diffusion barrier to liquid silicon [74,75].

Silicon nitride is another relevant ceramic material [54,71,159–161]. Its excellent properties, such as high hardness, low density, refractoriness and chemical inertness are used in many applications. These properties are mainly related to the strong Si–N bonds, with ~70% covalent character [162]. Silicon nitride provides an effective diffusion barrier and is compatible with SiC fibres and BN interphase for thermostructural applications. There are four allotropic forms of silicon nitride [163–166]:

- the hexagonal form α-Si_3N_4, consisting of a repetitive sequence of stacked atomic layers ABCD belonging to space group $P31_c$ (a = 0.7753 nm, c = 0.5618 nm) (ICDD PDF number: 04-005-5074),

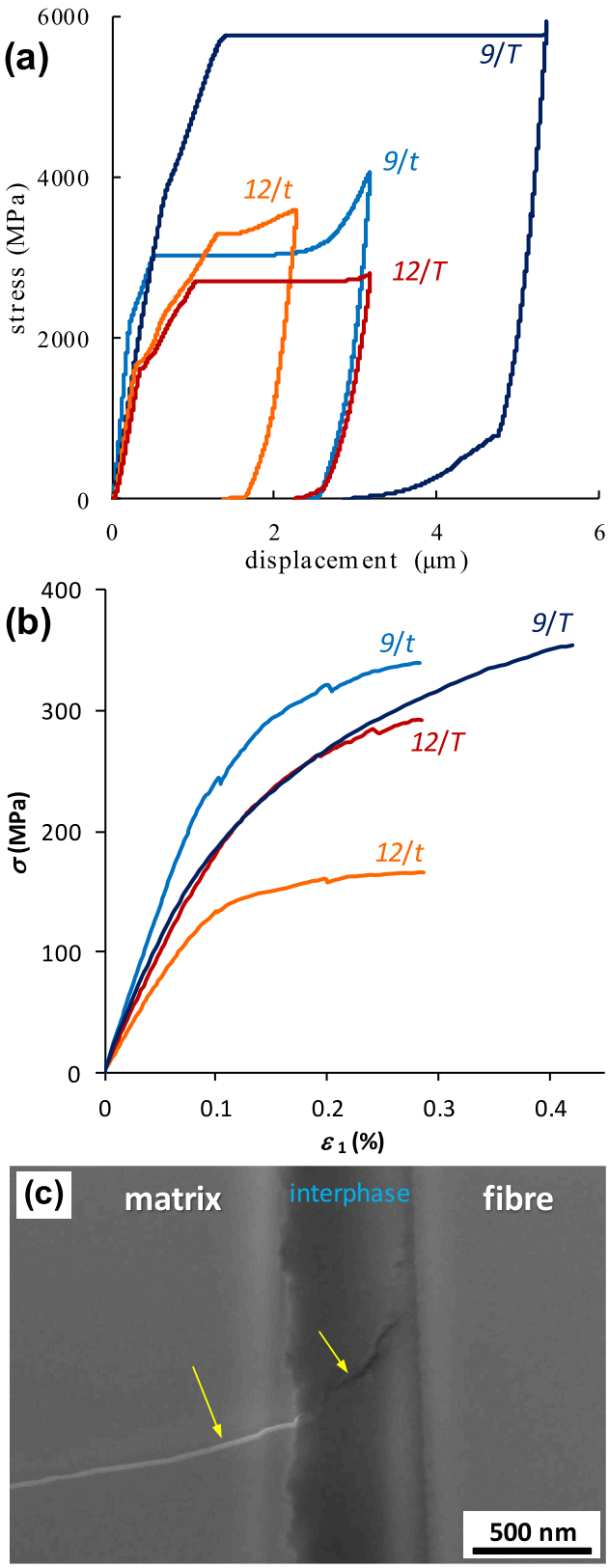

Fig. 9. (a) single-fibre push-out curves and (b) stress/strain curves obtained from tensile tests for single-ply composites with different BN interphases with low degree of crystallisation, thin (*9/t*) and thick (*9/T*), and with high degree of crystallisation, thin (*12/t*) and thick (*12/T*). (c) Focused ion beam - scanning electron microscope image of a crack (yellow arrows) deflected in a BN interphase *9/T* [158]. (For interpretation of the references to colour in this figure legend, the reader is referred to the Web version of this article.)

- the hexagonal form β-Si_3N_4, consisting of a repetitive sequence of stacked atomic layers AB belonging to space group $SP6_C/m$ (a = 0.7607 nm, c = 0.2911 nm) (ICDD PDF number: 01-076-0453),
- the cubic spinel structure c-Si_3N_4 resulting from extreme pressure and temperature conditions (P > 15 GPa, T > 2000 K),
- the amorphous form a-SiN_x, generally richer in silicon.

Hexagonal forms are particularly suitable for protection against oxidation and attack of silicon [167]. Thermal treatment allows a transition from the amorphous form to the α form and then to the β form. The α-β transition is slow and only occurs at 1400 °C in the presence of a liquid phase, otherwise at 1600 °C [162,165]. Si_3N_4 decomposes into Si and N_2 at low N_2 partial pressure and/or high temperature [167–170]. However, the vapour pressure of N_2 in ambient air at room temperature is sufficient to maintain a metastable state. The use of high N_2 pressures during heat treatment delays or prevents its decomposition [167].

The use of SiC or Si_3N_4 as a protective layer depends in particular on the synthesis variant chosen. The CVI process in a fibrous preform is used when the interphase itself has been synthesised by this process, in order to simplify the sequence of steps in the manufacture of the composite. Unlike SiC, the synthesis of Si_3N_4 by CVI has been little studied. SiC is therefore the natural choice. If the BN interphase has been synthesised by CVD on single fibre tows, the same process is likely to be used. The choice between SiC and Si_3N_4 then remains open.

6. Oxidation/corrosion behaviour of the fibre-matrix interfacial zone

6.1. Behaviour under dry air

The oxidation kinetics of boron nitride depends on its microstructure, structural anisotropy and the oxidising environment [121,123,151,171]. Several mechanisms are reported in the literature, depending on the by-products. In the presence of oxygen and above about 800 °C, it is generally accepted that sp^2-BN oxidises. Oxidation resistance up to 950 °C is observed for h-BN, while t-BN oxidises at lower temperatures [172–174]. Thus, a mass gain corresponding to the formation of B_2O_3, liquid from 410 to 450 °C, is observed according to Eq. 1:

$$4\ BN_{(s)} + 3\ O_{2(g)} \rightarrow 2\ B_2O_{3(l)} + 2\ N_{2(g)} \quad \text{Eq. 1}$$

The mass gain is linear with time as long as the oxide layer remains thin. It then follows a parabolic law as B_2O_3 forms a diffusion barrier to O_2 and slows down the process. This corresponds to case (a) in Fig. 10.

For SiC and Si_3N_4, a distinction is made between a passive and an active oxidation regime in the presence of O_2. In the general case, a solid passivating SiO_2 scale forms on the surface and limits and then stops the oxidation phenomenon (case (a) in Fig. 10). Oxidation is passive. However, at high temperature and very low oxygen pressure, volatile non-passivating SiO is formed at the expense of SiO_2 (Fig. 11) [170,175–177]. As the inward flux of O_2 diffusing to the SiC or Si_3N_4 surface becomes less than the outward flux of SiO diffusing to the bulk gas, oxygen is removed and a stable protective layer of SiO_2 cannot be formed. Oxidation therefore becomes active. Silicon nitride has up to 3 times slower oxidation kinetics than SiC. It is possible to describe the oxidation of silicon carbide and nitride according to the main oxidation mechanisms with Eqs. (2)–(5). Fig. 10 shows the 3 classical oxidation behaviours observed according to the balance between active and passive oxidation, depending on the conditions (temperature (T), partial pressure of O_2 (P_{O2}), etc.) [174,178].

$$Si_3N_{4(s)} + 3\ O_{2(g)} \rightarrow 3\ SiO_{2(s)} + 2\ N_{2(g)}\ \text{(passive)} \quad \text{Eq. 2}$$

$$2\ SiC_{(s)} + 3\ O_{2(g)} \rightarrow 2\ SiO_{2(s)} + 2\ CO_{(g)}\ \text{(passive)} \quad \text{Eq. 3}$$

$$2\ Si_3N_{4(s)} + 3\ O_{2(g)} \rightarrow 6\ SiO_{(g)} + 4\ N_{2(g)}\ \text{(active, high } T\text{, low } P_{O2}) \quad \text{Eq. 4}$$

$$SiC_{(s)} + O_{2(g)} \rightarrow SiO_{(g)} + CO_{(g)}\ \text{(active, high } T\text{, low } P_{O2}) \quad \text{Eq. 5}$$

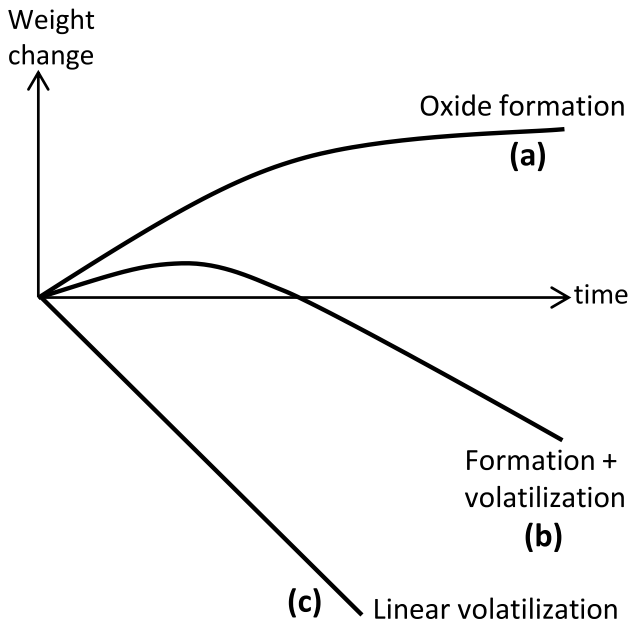

Fig. 10. Schematic behaviour curves for active or passive oxidation/corrosion kinetics [174].

6.2. Behaviour under wet air

Depending on the conditions used for gaseous route synthesis, poor stability of BN to moisture may occur [179]. This can be related to the hydration of B_2O_3, even at low temperatures, to form $H_xB_yO_z$. This instability is particularly significant when the deposition temperature of BN is limited, as required for I-CVI, and therefore the degree of crystallisation of BN is low. At 65 °C and after exposure times equal to or greater than 250 h, $H_xB_yO_z$ by-products can affect the BN/fibre interface and weaken the push-out behaviour of the composites [180]. In the case of thick BN coatings alone exposed to 800 °C and once saturated with hydrated species, volatilisation leading to active oxidation of the BN layer is observed according to a linear law (Fig. 10c) [123,174]. A similar effect can be observed for SiC with the formation of gaseous Si $(OH)_4$ at temperatures above 1200 °C. In the case of SiC/BN/SiC composites exposed to oxygen and moisture at temperatures above 500 °C, the active oxidation of BN results in a recession phenomenon with the removal of the interphase, which degrades the properties of the composite [181]. However, BN ex-I-CVI can be made less sensitive to moisture by a high temperature stabilisation treatment [142]. Furthermore, one of the advantages of using BN as a thin coating confined in a SiC or Si_3N_4 environment is the ability of B_2O_3 to dissolve SiO_2. A more stable borosilicate glass is then formed in a viscous/liquid state at high temperature in both dry and humid air. It provides crack healing in SiC/BN/SiC-SiB_x composites. The glass flows into the cracks and forms a high silica content seal that extends into the crack. It forms a barrier to the diffusion of oxidising species whose ability to limit the recession of the BN interphase depends on the partial pressure of water vapour and the temperature [123,181].

7. Interphase synthesis

Deposition by the gaseous route is generally used to uniformly coat fibres with a non-oxide interphase layer. This is because CVD/CVI processes allow the production of dense, high purity coatings over a suitable thickness range.

7.1. I-CVI batch process

The I-CVI batch process offers the possibility of producing the interphase in the same hot wall reactors as for the matrix or protective layers, thus avoiding its exposure to air, limiting the number of CMC production steps and allowing several parts to be treated simultaneously. Nevertheless, especially for BN, the processing conditions are limited by infiltration issues, with the need to use very low pressures (<10 mbar) and moderate temperatures (<1000 °C) to limit the infiltration gradients in the fibre preform and the risk of homogeneous phase nucleation [140,141]. However, significant thickness gradients remain, with thicker interphases at the surface than in the centre of the preform. In addition, BN coatings exhibit very low degrees of crystallisation at limited growth rates, of the order of only 0.1 μm/h. The infiltration conditions, often followed by a heat treatment (>1000 °C) [142,182], are the result of a compromise between (i) an acceptable deposition rate, (ii) a sufficient degree of crystallisation to ensure BN stability with respect to the ambient air, and (iii) a correct infiltration quality (low thickness gradient).

7.2. Continuous fibre tow coating

An alternative approach to the traditional I-CVI batch process is to deposit the interphase on the fibres prior to weaving. This is used, for example, in the "prepreg MI" variant of CMC production mentioned in section 3.5. In this type of continuous process, the multifilament tow is passed from spool to spool through a device to deposit the interphase. Nöth et al. have recently applied this principle to the wet chemical deposition of interphases [183]. However, the wet process is not as mature as the gaseous process, for which there are several earlier works on the continuous deposition of BN in hot wall CVD reactors [184–186]. The principle is illustrated in Fig. 12. Other coatings have also been deposited in this way, such as SiBN layers by Stöckel et al. [187] or SiBNC by Ye et al. [188]. The report by Corman and Luthra describes a

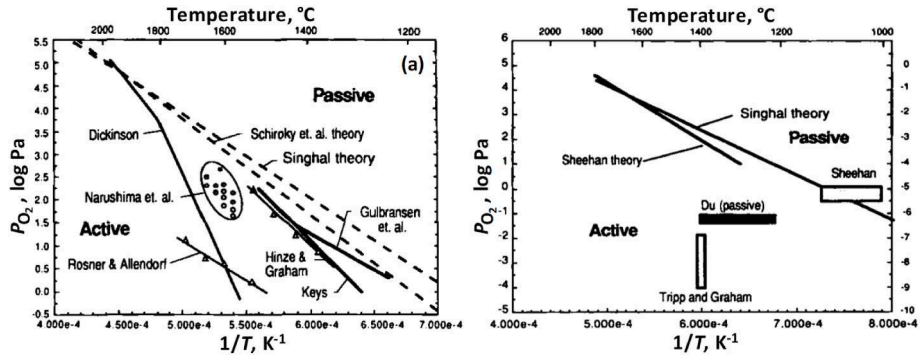

Fig. 11. Active-to-passive oxidation transition for SiC (a) and Si_3N_4 (b) [177].

continuous process for the deposition of BN, SiBN and Si_3N_4 thin films on Hi-Nicalon fibre tow, also by hot wall CVD [54].

Working directly on a tow overcomes the temperature and pressure limitations of CVI batch processes required for infiltration. Coating thickness gradients are also significantly reduced at equivalent temperatures, as precursor depletion and diffusion in the inter-fibre porosity extends only through the cross-section of a single tow, rather than through the thickness of an entire preform. When the conditions are well tuned, including limited fibre tow tension, the coatings obtained from this type of process have a more uniform thickness with low gradients between the core and the surface of the tow [186,189]. In addition, the higher synthesis temperatures achievable result in better crystallised coatings. The desired interphase thickness is achieved by adjusting the fibre tow feed speed. The tow speed is a crucial competitive criterion, the choice of which depends on the growth kinetics and the hot zone length. As with PyC [190], the continuous CVD process must achieve a higher local interphase growth rate than the I-CVI batch process in order to compete with the latter in terms of the volume of fibres processed, in a shorter time and in a smaller facility. An additional way to increase the throughput and reduce the production cost of the continuous process is to treat multiple tows passing through the same reactor simultaneously.

Today, one of the obstacles to further improvement of the continuous CVD process is the limited growth kinetics allowed by hot wall reactors. Indeed, even with improved film homogeneity compared to the I-CVI batch process, the problem of homogeneous phase nucleation remains critical at very high temperatures. It would therefore be interesting to develop a continuous CVD process on a SiC tow in a cold wall reactor. By limiting gas maturation, this reactor technology would achieve even higher growth rates and therefore higher tow feed speeds due to the higher processing temperatures allowed. By limiting the deposition on the reactor walls, a better yield can also be expected. This system has been implemented for carbon fibres [191] or SCS-6 (SiC fibre with a carbon core) [192], which can be heated directly by the Joule effect. However, due to the properties of SiC, inductive and resistive heating do not seem feasible for HNS fibres.

8. Precursors for CVD/CVI synthesis

8.1. BN precursors

Table 4 lists precursors that are or have been used to coat CMC reinforcing fibres by CVD/CVI, all in hot wall reactors. Other precursors used for CVD in general or even PECVD of BN could also be considered for interphase application in CMCs, such as hexachloroborazine [193] or those of the borane family [194–199]. Costs are based on prices obtained from laboratory suppliers for comparable quantities of about 100 g (where available). Obviously, precursors in industrial quantities, if available, are much cheaper. The cost of NH_3 is marginal compared to that of the boron precursors. The chemical elements present in these molecules other than boron and nitrogen have also been identified as potential sources of coating contamination (hydrogen, carbon, chlorine or fluorine).

Due to its relatively low cost, boron trichloride (BCl_3) combined with ammonia (NH_3) is the most commonly used precursor mixture for the industrial production of BN interphases. Depending on the conditions, BN is deposited following one or two reaction paths involving aminodichloroborane (Cl_2BNH_2) and dichloroborane ($BHCl_2$) as effective and intermediate precursors produced *in situ* in the CVD reactor [125]. These species influence the structural organisation of the deposited BN layers. The corrosive nature of the gaseous mixture and reaction by-products such as solid ammonium chloride (NH_4Cl), are responsible for additional facility costs (intensive maintenance, stainless materials, effluent treatment, etc.) [54]. Furthermore, when BCl_3 and NH_3 are mixed at room temperature, they readily form a stable complex ($Cl_3B{:}NH_3$) in the form of a powder [125,200]. These solids ($Cl_3B{:}NH_3$ and NH_4Cl) are detrimental to the operation of the system as they can block the cold gas inlets and outlets [54,125]. This gas mixture is therefore complex to implement.

The addition of ammonia to the boron precursor is common, even when the boron precursor itself is a nitrogen source. Indeed, NH_3 favours stoichiometric BN deposition by providing a high N/B ratio in the gas phase, compensating for any nitrogen deficiency in the coating. In addition, its high nitriding capacity allows the formation of $HCN_{(g)}$ in the presence of carbon, which significantly reduces carbon contamination in coatings deposited from carbonaceous precursors [156,191]. Although corrosive, NH_3 is much less aggressive than halide precursors. Materials used in CVD/CVI equipment must have good chemical resistance to this gas (elastomeric seals, etc.).

Table 4
Precursors for the synthesis of BN fibre coatings by CVD/CVI; sate at room temperature (RT); pressurised gas (Press.), inert atmosphere (IA), dry atmosphere (DA), cool place (CP) storage.

Precursor	Potential contamination	State at RT	Price (€/g)	Price (€/mol BN)	Storage
Borazine [188,201,202]	H	Liquid	50	1300	<5 °C - IA
Ammonia borane [203]	H	Solid	22	679	CP - IA
Diborane + ammonia [160]	H	Gas			Press.
Tris (dimethylamino) borane + ammonia [156,191]	H, C	Liquide	12	1770	IA
Trichloroborazine [204,205]	H, Cl	Solid	2860	175000	CP - DA
Boron trifluoride + ammonia [155,206–208]	H, F	Gas	3.7	247	Press.
Boron trichloride + ammonia [68,125,139,142,158,208,209]	H, Cl	Gas	0.3	32	Press.

8.2. SiC and Si_3N_4 precursors

The precursors used or studied for the synthesis of SiC and Si_3N_4 by CVD/CVI in CMCs are mainly chlorosilanes. They are listed in Table 5.

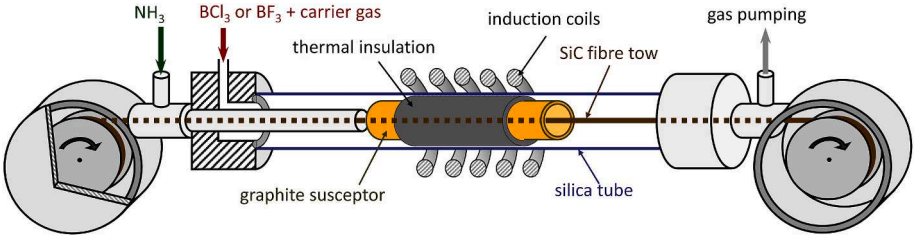

Fig. 12. Schematic illustration of continuous CVD fibre tow coating equipment [185].

Their corrosive nature entails additional costs for the deposition equipment (maintenance, effluent treatment, etc.). On the other hand, they are cheap, which is even more crucial in the case of matrix production, since the matrix represents a larger part of the composite than the interphase. Additional interest has been shown in MTS, a precursor widely used for SiC in the CMC industry, but generalisable to other chlorosilanes. The derived HCl by-product can help to suppress free Si deposition during the growth of SiC films or crystals [94]. Hydrogen is also used as a carrier gas as it promotes the reduction of Si-Cl bonds on the growing SiC surface. The reaction paths leading to the deposition of SiC typically involve several complex gas phase maturation sub-reactions [210,211].

For Si_3N_4, the nitrogen source added to the chlorosilane is almost always NH_3 due to its high reactivity even at low temperatures. The formation of the solid by-product NH_4Cl at low temperatures is also critical to the process.

9. Summary and outlook

SiC/SiC CMCs reinforced with the latest generation of continuous fibres are technical materials that are complex to process but are suitable for thermostructural applications, particularly in aircraft engines. The various steps in their manufacture require heavy and expensive processes which have had to be adapted to industrial mass production and which have a strong influence on the properties of the final parts. Today, MI/RMI processes complement the CVI synthesis of the SiC matrix to make it denser and increase the stiffness of the composite. The disadvantage is the presence of residual free silicon. To further increase the operating temperature of CMCs, it will be necessary to obtain both a dense and pure SiC matrix. The current production difficulties are offset by the reduction in energy consumption achieved by the use of these continuous fibre reinforced composites due to their refractoriness and lightness. Recent advances such as the development of new fibres, the simplification of matrix synthesis and the development of EBCs are promising for the future. The interphase, which is a key component in the damage tolerance of CMCs, and its proper control contribute to their success.

The sp^2-BN interphases provide a mechanical fuse function with better resistance to ambient oxidation and liquid silicon attack than PyC interphases. One of the advantages of BN interphases is the occurrence of a healing mechanism during oxidation/corrosion of a SiC/SiC CMC at high temperatures. However, they must be covered with a protective coating, ideally SiC or Si_3N_4, before the matrix is produced by the MI process.

The interphase and its protective coating can be produced either by the I-CVI batch process or by continuous CVD coating of the fibre tow in hot wall reactors. The former is confronted with infiltration gradients that must be limited by the use of moderate temperatures. To be competitive, i.e. to be able to treat large quantities of fibres in reasonably sized facilities, the latter must be able to achieve high coating growth rates by using high temperatures. These conditions have the added benefit of producing a boron nitride with a high degree of crystallinity, giving it a higher intrinsic stability to moist air, even at low temperatures.

One way to further improve the continuous CVD process would be to use of a cold wall reactor to limit homogeneous phase nucleation. However, conventional heaters are not suitable for SiC fibres. In this case, where the fibre tows move continuously in the reactor and in the gas phase, the use of non-contact heating would be ideal, but remains to be identified and tested. In addition, alternative precursors to the usual chlorosilanes will have to be used, as otherwise the problems associated with the production of solid chlorinated by-products in the cold wall reactor will be exacerbated.

Table 5
Chloride precursors for the synthesis of SiC and Si_3N_4 by CVD/CVI (inert atmosphere (IA), cool place (CP)).

Precursor	State at RT	Price (€/g)	Price (€/molSiC)	Storage
for SiC				
Methyltrichlorosilane [82,94,212–215]	Liquid	0.5	70	CP - IA
Vinyltrichlorosilane [93]	Liquid	0.3	43	2–8 °C - IA
Dichloromethylsilane [216]	Liquid (<41 °C)	0.4	42	2–8 °C - IA
Dichlorodimethylsilane [217,218]	Liquid	0.4	49	2–8 °C - IA
Silicon tetrachloride + methane [219,220]	Liquid	0.4	75	IA
for Si_3N_4			(€/molSi_3N_4)	
Dichlorosilane + ammonia [221,222]	Liquid	1.4	420	IA
Trichlorosilane + ammonia [54,71]	Liquid	0.4	180	2–8 °C - IA
Silicon tetrachloride + ammonia [223–225]	Liquid	0.4	230	IA
Hexachlorodisilane + ammonia [226,227]	Liquid	27	11000	CP - IA

Declaration of competing interest

The authors declare that they have no known competing financial interests or personal relationships that could have appeared to influence the work reported in this paper.

Acknowledgements

P. Fenetaud was supported by SAFRAN CERAMICS through a PhD grant while writing this overview.

References

[1] European Union, Clean sky 2 - clean aviation, n.d. https://www.clean-aviation.eu/clean-sky-2. (Accessed 24 June 2022).
[2] G. Karadimas, K. Salonitis, Ceramic matrix composites for aero engine applications—a review, Appl. Sci. 13 (2023) 3017, https://doi.org/10.3390/app13053017.
[3] E. Bouillon, N. Laval, D. Marsal, in: Y. Kagawa, R. Darolia, R. Raj (Eds.), SiC-based Ceramic Matrix Composite Behavior Enhancement for Gas Turbines Hot Sections, 2017. https://dc.engconfintl.org/acmc/47/. (Accessed 8 July 2022).
[4] G.S. Corman, K.L. Luthra, 5.13 development history of GE's prepreg melt infiltrated ceramic matrix composite material and applications, in: Comprehensive Composite Materials II, Elsevier, 2018, pp. 325–338, https://doi.org/10.1016/B978-0-12-803581-8.10001-3.
[5] W. White, 1.1 Basic science of advanced ceramics, in: Handbook of Advanced Ceramics, Elsevier, 2003, pp. 3–80, https://doi.org/10.1016/B978-012654640-8/50003-1.
[6] J.E. Grady, Recent progress and future directions for CMC research and development at NASA glenn, in: Fundamental Aeronautics Program 2012 Technical Conference, 2012.
[7] A.K. Misra, Durability challenges for next generation of gas turbine engine materials, Biarritz, https://ntrs.nasa.gov/citations/20130010776, 2012. (Accessed 24 June 2022).
[8] N.P. Padture, Advanced structural ceramics in aerospace propulsion, Nat. Mater. 15 (2016) 804–809, https://doi.org/10.1038/nmat4687.
[9] J. Steibel, Ceramic matrix composites taking flight at GE aviation, Am. Ceram. Soc. Bull. 98 (2019) 30–33.
[10] D. Zhu, Aerospace ceramic materials: thermal, environmental barrier coatings and SiC/SiC ceramic matrix composites for turbine engine applications, n.d, https://ntrs.nasa.gov/citations/20180002984.
[11] X. Wang, X. Gao, Z. Zhang, L. Cheng, H. Ma, W. Yang, Advances in modifications and high-temperature applications of silicon carbide ceramic matrix composites in aerospace: a focused review, J. Eur. Ceram. Soc. 41 (2021) 4671–4688, https://doi.org/10.1016/j.jeurceramsoc.2021.03.051.
[12] R. Naslain, Fibrous ceramic-ceramic composite materials processing and properties, J. Phys. Colloq. 47 (1986), https://doi.org/10.1051/jphyscol:19861107. C1-703-C1-715.

[13] R.R. Naslain, The design of the fibre-matrix interfacial zone in ceramic matrix composites, Compos. Appl. Sci. Manuf. 29 (1998) 1145–1155, https://doi.org/10.1016/S1359-835X(97)00128-0.

[14] G. Camus, C. Lorrette, R. Pailler, F. Rebillat, B. Reignier, F. Teyssandier, Ceramic matrix composite materials with long fibers reinforcement, Éditions techniques de l'ingénieur. https://doi.org/10.51257/a-v2-n4803, 2016. (Accessed 24 June 2022).

[15] G.W. Brassell, J.A. Horak, B.L. Butler, Effects of porosity on strength of carbon-carbon composites, J. Compos. Mater. 9 (1975) 288–296, https://doi.org/10.1177/002199837500900307.

[16] N. Eswara Prasad, Anil Kumar, J. Subramanyam, Ceramic matrix composites (CMCs) for aerospace applications, in: N. Eswara Prasad, R.J.H. Wanhill (Eds.), Aerospace Materials and Material Technologies, Springer Singapore, Singapore, 2017, pp. 371–389, https://doi.org/10.1007/978-981-10-2134-3_16.

[17] S. Yajima, K. Okamura, J. Hayashi, M. Omori, Synthesis of continuous SiC fibers with high tensile strength, J. Am. Ceram. Soc. 59 (1976) 324–327, https://doi.org/10.1111/j.1151-2916.1976.tb10975.x.

[18] R. Naslain, P. Hagenmuller, F. Christin, L. Heraud, J.J. Choury, The carbon fiber-carbon and silicon carbide binary matrix composites a new class of materials for high temperature applications, in: Advances in Composite Materials, Elsevier, 1980, pp. 1084–1097, https://doi.org/10.1016/B978-1-4832-8370-8.50087-5.

[19] D.M. Levy, Ceramic matrix composites take flight in LEAP jet engine. https://www.ornl.gov/news/ceramic-matrix-composites-take-flight-leap-jet-engine, 2017. (Accessed 5 April 2023).

[20] P. Bradley, N. Hurn, GE9X engine achieves FAA certification. https://www.ge.com/news/press-releases/ge9x-engine-achieves-faa-certification, 2020. (Accessed 5 April 2023).

[21] V. Haase, G. Kirschstein, H. List, S. Ruprecht, R. Sangster, F. Schröder, W. Töpper, H. Vanecek, W. Heit, J. Schlichting, H. Katscher, The Si-C phase diagram, in: H. Katscher, R. Sangster, F. Schröder (Eds.), Si Silicon, Springer Berlin Heidelberg, Berlin, Heidelberg, 1985, pp. 1–5, https://doi.org/10.1007/978-3-662-06994-3_1.

[22] M. Dubey, G. Singh, G. Van Tendeloo, X-ray diffraction and transmission electron microscopy study of extremely large-period polytypes in SiC, Acta Crystallogr. A. 33 (1977) 276–279, https://doi.org/10.1107/S0567739477000692.

[23] L.U. Ogbuji, Origin of long-period polytypism in polycrystalline SiC, phys. stat. sol. (a). 72 (1982) 455–461, https://doi.org/10.1002/pssa.2210720203.

[24] G.R. Fisher, P. Barnes, Towards a unified view of polytypism in silicon carbide, Phil. Mag. B 61 (1990) 217–236, https://doi.org/10.1080/13642819008205522.

[25] T. Kimoto, J.A. Cooper, Physical properties of silicon carbide, in: Fundamentals of Silicon Carbide Technology: Growth, Characterization, Devices, and Applications, John Wiley & Sons Singapore Pte. Ltd, Singapore, 2014, pp. 11–38, https://doi.org/10.1002/9781118313534.ch2.

[26] K.A. Schwetz, Silicon carbide based hard materials, in: R. Riedel (Ed.), Handbook of Ceramic Hard Materials, Wiley-VCH Verlag GmbH, Weinheim, Germany, 2000, pp. 683–748, https://doi.org/10.1002/9783527618217.ch20.

[27] G.L. Harris, Institution of electrical engineers, in: Properties of Silicon Carbide, INSPEC, the Inst. of Electrical Engineers, London, 1995.

[28] V.J. Jennings, The etching of silicon carbide, in: Silicon Carbide–1968, Elsevier, 1969, pp. S199–S210, https://doi.org/10.1016/B978-0-08-006768-1.50023-1.

[29] F. Galasso, M. Basche, D. Kuehl, Preparation, structure and properties of continuous silicon carbide filaments, Appl. Phys. Lett. 9 (1966) 37–39, https://doi.org/10.1063/1.1754590.

[30] D.A. Scola, C.S. Brooks, Surface aspects of new fibers, boron, silicon carbide, and graphite, J. Adhes. 2 (1970) 213–237, https://doi.org/10.1080/0021846708544594.

[31] S. Yajima, J. Hayashi, M. Omori, Continuous silicon carbide fiber of high tensile strength, Chem. Lett. 4 (1975) 931–934, https://doi.org/10.1246/cl.1975.931.

[32] S. Yajima, Y. Hasegawa, J. Hayashi, M. Iimura, Synthesis of continuous silicon carbide fibre with high tensile strength and high Young's modulus: Part 1 Synthesis of polycarbosilane as precursor, J. Mater. Sci. 13 (1978) 2569–2576, https://doi.org/10.1007/PL00020149.

[33] Y. Hasegawa, M. Iimura, S. Yajima, Synthesis of continuous silicon carbide fibre: Part 2 Conversion of polycarbosilane fibre into silicon carbide fibres, J. Mater. Sci. 15 (1980) 720–728, https://doi.org/10.1007/BF00551739.

[34] A.R. Bunsell, M.-H. Berger, Fine diameter ceramic fibres, J. Eur. Ceram. Soc. 20 (2000) 2249–2260, https://doi.org/10.1016/S0955-2219(00)00090-X.

[35] D. Schawaller, B. Clauß, M.R. Buchmeiser, Ceramic filament fibers - a review, Macromol. Mater. Eng. 297 (2012) 502–522, https://doi.org/10.1002/mame.201100364.

[36] P. Wang, F. Liu, H. Wang, H. Li, Y. Gou, A review of third generation SiC fibers and SiC_f/SiC composites, J. Mater. Sci. Technol. 35 (2019) 2743–2750, https://doi.org/10.1016/j.jmst.2019.07.020.

[37] H. Ichikawa, Advances in SiC fibers for high temperature applications, in: Advanced Inorganic Fibrous Composites V, Trans Tech Publications Ltd, 2006, pp. 17–23. https://doi.org/10.4028/www.scientific.net/AST.50.17.

[38] H. Ichikawa, Recent advances in Nicalon ceramic fibres including Hi-Nicalon type S, Ann. Chim. Sci. Mat. 25 (2000) 523–528, https://doi.org/10.1016/S0151-9107(01)80004-0.

[39] J.J. Sha, T. Nozawa, J.S. Park, Y. Katoh, A. Kohyama, Effect of heat treatment on the tensile strength and creep resistance of advanced SiC fibers, J. Nucl. Mater. 329–333 (2004) 592–596, https://doi.org/10.1016/j.jnucmat.2004.04.123.

[40] J.J. Sha, T. Hinoki, A. Kohyama, Microstructure and mechanical properties of Hi-Nicalon^{TM} Type S fibers annealed and crept in various oxygen partial pressures, Mater. Char. 60 (2009) 796–802, https://doi.org/10.1016/j.matchar.2009.01.017.

[41] J.A. DiCarlo, Advances in SiC/SiC composites for aero-propulsion, in: N.P. Bansal, J. Lamon (Eds.), Ceramic Matrix Composites: Materials, Modeling and Technology, John Wiley & Sons, Inc., Hoboken, NJ, USA, 2014, pp. 217–235, https://doi.org/10.1002/9781118832998.ch7.

[42] M. Takeda, J. Sakamoto, A. Saeki, H. Ichikawa, Mechanical and structural analysis of silicon carbide fiber Hi-Nicalon Type S, in: J.B. Wachtman (Ed.), Ceramic Engineering and Science Proceedings, John Wiley & Sons, Inc., Hoboken, NJ, USA, 1996, pp. 35–42, https://doi.org/10.1002/9780470314876.ch2.

[43] G. Chollon, R. Pailler, R. Naslain, F. Laanani, M. Monthioux, P. Olry, Thermal stability of a PCS-derived SiC fibre with a low oxygen content (Hi-Nicalon), J. Mater. Sci. 32 (1997) 327–347, https://doi.org/10.1023/A:1018541030308.

[44] T. Tanaka, S. Shibayama, M. Takeda, A. Yokoyama, Recent progress of hi-nicalon type S development, in: W.M. Kriven, H.-T. Lin (Eds.), Ceramic Engineering and Science Proceedings, John Wiley & Sons, Inc., Hoboken, NJ, USA, 2003, pp. 217–223, https://doi.org/10.1002/9780470294826.ch32.

[45] T. Morimoto, T. Ogasawara, Potential strength of Nicalon^{TM}, Hi Nicalon^{TM}, and Hi Nicalon type S^{TM} monofilaments of variable diameters, Composites Part A Appl. Sci. Manuf. 37 (2006) 405–412, https://doi.org/10.1016/j.compositesa.2005.05.046.

[46] J.J. Sha, T. Hinoki, A. Kohyama, Thermal and mechanical stabilities of Hi-Nicalon SiC fiber under annealing and creep in various oxygen partial pressures, Corrosion Sci. 50 (2008) 3132–3138, https://doi.org/10.1016/j.corsci.2008.08.003.

[47] R.T. Bhatt, F. Sola', L.J. Evans, R.B. Rogers, D.F. Johnson, Microstructural, strength, and creep characterization of Sylramic^{TM}, Sylramic^{TM}-iBN and super Sylramic^{TM}-iBN SiC fibers, J. Eur. Ceram. Soc. 41 (2021) 4697–4709, https://doi.org/10.1016/j.jeurceramsoc.2021.03.024.

[48] S.M. Dong, G. Chollon, C. Labrugère, M. Lahaye, A. Guette, J.L. Bruneel, M. Couzi, R. Naslain, D.L. Jiang, Characterization of nearly stoichiometric SiC ceramic fibres, J. Mater. Sci. 36 (2001) 2371–2381, https://doi.org/10.1023/A:1017988827616.

[49] A.R. Bunsell, A. Piant, A review of the development of three generations of small diameter silicon carbide fibres, J. Mater. Sci. 41 (2006) 823–839, https://doi.org/10.1007/s10853-006-6566-z.

[50] J. Lipowitz, J.A. Rabe, A. Zangvil, Y. Xu, Structure and properties of Sylramic^{TM} silicon carbide fiber—a polycrystalline, stoichiometric β-SiC composition, in: J. P. Singh (Ed.), Ceramic Engineering and Science Proceedings, John Wiley & Sons, Inc., Hoboken, NJ, USA, 1997, pp. 147–157, https://doi.org/10.1002/9780470294437.ch16.

[51] H. Spilker, HI-NICALON^{TM} type S SiC fiber, n.d. https://www.coiceramics.com/pdfs/Hi-Nicalon-Type-S.pdf. (Accessed 4 July 2022).

[52] R. Kamiya, B.A. Cheeseman, P. Popper, T.-W. Chou, Some recent advances in the fabrication and design of three-dimensional textile preforms: a review, Compos. Sci. Technol. 60 (2000) 33–47, https://doi.org/10.1016/S0266-3538(99)00093-7.

[53] M. Ansar, W. Xinwei, Z. Chouwei, Modeling strategies of 3D woven composites: a review, Compos. Struct. 93 (2011) 1947–1963, https://doi.org/10.1016/j.compstruct.2011.03.010.

[54] G.S. Corman, K.L. Luthra, Melt infiltrated ceramic composites (Hipercomp) for gas turbine engine applications. https://doi.org/10.2172/936318, 2006.

[55] M. Omori, H. Takei, Pressureless sintering of SiC, J. Am. Ceram. Soc. 65 (1982), https://doi.org/10.1111/j.1151-2916.1982.tb10460.x c92–c92.

[56] S. Dong, Y. Katoh, A. Kohyama, Preparation of SiC/SiC composites by hot pressing, using Tyranno-SA fiber as reinforcement, J. Am. Ceram. Soc. 86 (2003) 26–32, https://doi.org/10.1111/j.1151-2916.2003.tb03272.x.

[57] K. Shimoda, T. Hinoki, A. Kohyama, Effect of additive content on transient liquid phase sintering in SiC nanopowder infiltrated SiCf/SiC composites, Compos. Sci. Technol. 71 (2011) 609–615, https://doi.org/10.1016/j.compscitech.2010.12.014.

[58] Y. Katoh, A. Kohyama, J.-J. Kai, S. Dong, T. Hinoki, Microstructure and properties of liquid phase sintered SiC/SiC composites, in: H.-T. Lin, M. Singh (Eds.), Ceramic Engineering and Science Proceedings, John Wiley & Sons, Inc., Hoboken, NJ, USA, 2002, pp. 362–370, https://doi.org/10.1002/9780470294741.ch42.

[59] J.-B. Veyret, P. Tambuyser, C. Olivier, E. Bullock, M.-H. Vidal-Setif, Hi-Nicalon reinforced silicon nitride matrix composites, J. Mater. Sci. 32 (1997) 3457–3462, https://doi.org/10.1023/A:1018680919057.

[60] F. Guillard, A. Allemand, J.-D. Lulewicz, J. Galy, Densification of SiC by SPS-effects of time, temperature and pressure, J. Eur. Ceram. Soc. 27 (2007) 2725–2728, https://doi.org/10.1016/j.jeurceramsoc.2006.10.005.

[61] K. Nakano, A. Kamiya, Y. Nishino, T. Imura, T.-W. Chou, Fabrication and characterization of three-dimensional carbon fiber reinforced silicon carbide and silicon nitride composites, J. Am. Ceram. Soc. 78 (1995) 2811–2814, https://doi.org/10.1111/j.1151-2916.1995.tb08058.x.

[62] C.A. Nannetti, A. Ortona, D.A. Pinto, B. Riccardi, Manufacturing SiC-fiber-reinforced SiC matrix composites by improved CVI/slurry infiltration/polymer impregnation and pyrolysis, J. Am. Ceram. Soc. 87 (2004) 1205–1209, https://doi.org/10.1111/j.1551-2916.2004.tb20093.x.

[63] S.-H. Lee, M. Weinmann, F. Aldinger, Fabrication of fiber-reinforced ceramic composites by the modified slurry infiltration technique, J. Am. Ceram. Soc. 90 (2007) 2657–2660, https://doi.org/10.1111/j.1551-2916.2007.01795.x.

[64] D. Brewer, HSR/EPM combustor materials development program, Mater. Sci. Eng. 261 (1999) 284–291, https://doi.org/10.1016/S0921-5093(98)01079-X.

[65] J.J. Brennan, Interfacial characterization of a slurry-cast melt-infiltrated SiC/SiC ceramic-matrix composite, Acta Mater. 48 (2000) 4619–4628, https://doi.org/10.1016/S1359-6454(00)00248-2.

[66] M. Takeda, Y. Kagawa, S. Mitsuno, Y. Imai, H. Ichikawa, Strength of a Hi-Nicalon^{TM}/silicon-carbide-matrix composite fabricated by the multiple polymer infiltration-pyrolysis process, J. Am. Ceram. Soc. 82 (1999) 1579–1581, https://doi.org/10.1111/j.1151-2916.1999.tb01960.x.

[67] G. Zheng, H. Sano, Y. Uchiyama, K. Kobayashi, K. Suzuki, H. Cheng, Preparation and fracture behavior of carbon fiber/SiC composites by multiple impregnation and pyrolysis of polycarbosilane, J. Ceram. Soc. Japan. 106 (1998) 1155–1161, https://doi.org/10.2109/jcersj.106.1155.

[68] K.L. Luthra, G.S. Corman, Melt infiltrated (MI) SiC/SiC composites for gas turbine applications, in: W. Krenkel, R. Naslain, H. Schneider (Eds.), High Temperature Ceramic Matrix Composites, Wiley-VCH Verlag GmbH & Co. KGaA, Weinheim, FRG, 2006, pp. 744–753, https://doi.org/10.1002/3527605622.ch113.

[69] A. Marchais, D. Vicien, E. Mendez, J. Roger, Method for Infiltrating a Porous Preform, patent WO2018162829, 2018.

[70] R. Naslain, Design, preparation and properties of non-oxide CMCs for application in engines and nuclear reactors: an overview, Compos. Sci. Technol. 64 (2004) 155–170, https://doi.org/10.1016/S0266-3538(03)00230-6.

[71] B. Cossou, S. Jacques, G. Couégnat, S.W. King, L. Li, W.A. Lanford, G. Bhattarai, M. Paquette, G. Chollon, Synthesis and optimization of low-pressure chemical vapor deposition-silicon nitride coatings deposited from $SiHCl_3$ and NH_3, Thin Solid Films 681 (2019) 47–57, https://doi.org/10.1016/j.tsf.2019.04.045.

[72] R.N. Singh, A.R. Gaddipati, Composite Containing Coated Fibrous Material, Patent US4981822, 1991.

[73] B. Mainzer, K. Kelm, P. Watermeyer, M. Frieß, D. Koch, How to tame the aggressiveness of liquid silicon in the LSI process, Key Eng. Mater. 742 (2017) 238–245. https://doi.org/10.4028/www.scientific.net/KEM.742.238.

[74] I. Berdoyes, Interactions entre le silicium liquide et le carbure de silicium, application au composite SiC/SiC, PhD, University of Bordeaux, 2018. http://www.theses.fr/2018BORD0113.

[75] B. Mainzer, R. Jemmali, P. Watermeyer, K. Kelm, M. Frieß, D. Koch, Development of damage-tolerant ceramic matrix composites (SiC/SiC) using Si-BN/SiC/pyC fiber coatings and LSI processing, J. Ceram. Sci. Technol. 8 (2017) 113–120, https://doi.org/10.4416/JCST2016-00095.

[76] E.O. Einset, Analysis of reactive melt infiltration in the processing of ceramics and ceramic composites, Chem. Eng. Sci. 53 (1998) 1027–1039, https://doi.org/10.1016/S0009-2509(97)00379-5.

[77] P.J. Hofbauer, F. Raether, E. Rädlein, Finite element modeling of reactive liquid silicon infiltration, J. Eur. Ceram. Soc. 40 (2020) 251–258, https://doi.org/10.1016/j.jeurceramsoc.2019.09.041.

[78] T.J. Whalen, A.T. Anderson, Wetting of SiC, Si_3N_4, and carbon by Si and binary Si alloys, J. Am. Ceram. Soc. 58 (1975) 396–399, https://doi.org/10.1111/j.1151-2916.1975.tb19006.x.

[79] K. Mukai, Z. Yuan, Wettability of ceramics with molten silicon at temperatures ranging from 1693 to 1773 K, Mater. Trans., JIM 41 (2000) 338–345, https://doi.org/10.2320/matertrans1989.41.338.

[80] Z. Yuan, W.L. Huang, K. Mukai, Wettability and reactivity of molten silicon with various substrates, Appl. Phys. A 78 (2004) 617–622, https://doi.org/10.1007/s00339-002-2001-8.

[81] G.W. Liu, M.L. Muolo, F. Valenza, A. Passerone, Survey on wetting of SiC by molten metals, Ceram. Int. 36 (2010) 1177–1188, https://doi.org/10.1016/j.ceramint.2010.01.001.

[82] F. Langlais, G.L. Vignoles, 5.4 chemical vapor infiltration processing of ceramic matrix composites, in: Comprehensive Composite Materials II, Elsevier, 2018, pp. 86–129, https://doi.org/10.1016/B978-0-12-803581-8.03912-6.

[83] T.M. Besmann, D.P. Stinton, R.A. Lowden, W.Y. Lee, Chemical vapor deposition (CVD) and infiltration (CVI), in: A.W. Weimer (Ed.), Carbide, Nitride and Boride Materials Synthesis and Processing, Springer, Dordrecht, Netherlands, 1997, pp. 547–577, https://doi.org/10.1007/978-94-009-0071-4_22.

[84] I. Golecki, Rapid vapor-phase densification of refractory composites, Mater. Sci. Eng. R Rep. 20 (1997) 37–124, https://doi.org/10.1016/S0927-796X(97)00003-X.

[85] T. Belmonte, Dépôts chimiques à partir d'une phase gazeuse, Éditions techniques de l'ingénieur. https://doi.org/10.51257/a-v2-m1660, 2010. (Accessed 6 July 2022).

[86] J.-O. Carlsson, P.M. Martin, Chemical vapor deposition, in: Handbook of Deposition Technologies for Films and Coatings, Elsevier, 2010, pp. 314–363, https://doi.org/10.1016/B978-0-8155-2031-3.00007-7.

[87] H. Frey, Chemical vapor deposition (CVD), in: H. Frey, H.R. Khan (Eds.), Handbook of Thin-Film Technology, Springer Berlin Heidelberg, Berlin, Heidelberg, 2015, pp. 225–252, https://doi.org/10.1007/978-3-642-05430-3_9.

[88] W.E. Sawyer, A. Man, Improvement in carbons for electrics lights, Patent US211262 (1879).

[89] W.E. Sawyer, A. Man, Carbon for electric lights, Patent US229335 (1880).

[90] F.H. Pollard, P. Woodward, The growth of titanium nitride on hot filaments, J. Chem. Soc. (1948) 1709–1713, https://doi.org/10.1039/jr9480001709.

[91] S. Arrhenius, Über die Reaktionsgeschwindigkeit bei der Inversion von Rohrzucker durch Säuren, Z. Phys. Chem. 4U (1889) 226–248, https://doi.org/10.1515/zpch-1889-0416.

[92] K.J. Laidler, The development of the Arrhenius equation, J. Chem. Educ. 61 (1984) 494–498, https://doi.org/10.1021/ed061p494.

[93] A. Desenfant, G. Laduye, G.L. Vignoles, G. Chollon, Kinetic and gas-phase study of the chemical vapor deposition of silicon carbide from $C_2H_3SiCl_3/H_2$, J. Ind. Eng. Chem. 94 (2021) 145–158, https://doi.org/10.1016/j.jiec.2020.10.029.

[94] A. Lazzeri, CVI processing of ceramic matrix composites, in: N.P. Bansal, A. R. Boccaccini (Eds.), Ceramics and Composites Processing Methods, John Wiley & Sons, Inc., Hoboken, NJ, USA, 2012, pp. 313–349, https://doi.org/10.1002/9781118176665.ch9.

[95] F. Christin, Plant for the Chemical Infiltration in Vapor Phase of a Refractory Material Other than Carbon, Patent WO8704733, 1987.

[96] M. Montaudon, E. Bouillon, in: Y. Kagawa, D. Zhu, R. Darolia, R. Raj (Eds.), High Temperature Composite Overview in France, 2017. https://dc.engconfintl.org/acmc/59. (Accessed 7 July 2022).

[97] C. Sasso, Photograph of the top of a CVI facility at safran landing system in villeurbanne, France, for the production of C/C composites. https://medialibrary.safran-group.com/Photos/media/241816, 2018. (Accessed 16 December 2022).

[98] A. D'Angio, Microwave Enhanced Chemical Vapour Infiltration of Silicon Carbide Fibre Preforms, PhD, University of Birmingham, UK, 2018. https://etheses.bham.ac.uk/id/eprint/8188/.

[99] R. D'Ambrosio, L. Aliotta, V. Gigante, M.B. Coltelli, G. Annino, A. Lazzeri, Design of a pilot-scale microwave heated chemical vapor infiltration plant: an innovative approach, J. Eur. Ceram. Soc. 41 (2021) 3019–3029, https://doi.org/10.1016/j.jeurceramsoc.2020.05.073.

[100] E. Bouillon, F. Abbe, S. Goujard, E. Pestourie, G. Habarou, B. Dambrine, Mechanical and thermal properties of a self-sealing matrix composite and determination of the life time duration, in: T. Jessen, E. Ustundag (Eds.), Ceramic Engineering and Science Proceedings, John Wiley & Sons, Inc., Hoboken, NJ, USA, 2000, pp. 459–467, https://doi.org/10.1002/9780470294628.ch54.

[101] K.N. Lee, Environmental barrier coatings for SiC_f/SiC, in: N.P. Bansal, J. Lamon (Eds.), Ceramic Matrix Composites, John Wiley & Sons, Inc., Hoboken, NJ, USA, 2014, pp. 430–451, https://doi.org/10.1002/9781118832998.ch15.

[102] G. Corman, R. Upadhyay, S. Sinha, S. Sweeney, S. Wang, S. Biller, K. Luthra, General electric company: selected applications of ceramics and composite materials, in: L.D. Madsen, E.B. Svedberg (Eds.), Materials Research for Manufacturing, Springer International Publishing, Cham, 2016, pp. 59–91, https://doi.org/10.1007/978-3-319-23419-9_3.

[103] A. Evans, F. Zok, J. Davis, The role of interfaces in fiber-reinforced brittle matrix composites, Compos. Sci. Technol. 42 (1991) 3–24, https://doi.org/10.1016/0266-3538(91)90010-M.

[104] K.K. Chawla, Interface mechanics and toughness, in: Ceramic Matrix Composites, Springer US, Boston, MA, 1993, pp. 291–339, https://doi.org/10.1007/978-1-4757-2216-1_9.

[105] A.G. Evans, F.W. Zok, The physics and mechanics of fibre-reinforced brittle matrix composites, J. Mater. Sci. 29 (1994) 3857–3896, https://doi.org/10.1007/BF00355946.

[106] R.R. Naslain, R.J.-F. Pailler, J.L. Lamon, Single- and multilayered interphases in SiC/SiC composites exposed to severe environmental conditions: an overview: layered interphases in SiC/SiC composites, Int. J. Appl. Ceram. Technol. 7 (2010) 263–275, https://doi.org/10.1111/j.1744-7402.2009.02424.x.

[107] J. Lamon, Interfaces and interfacial mechanics : influence on the mechanical behavior of ceramic matrix composites (CMC), J. Phys. IV France. 3 (1993), https://doi.org/10.1051/jp4:19937252. C7-1607-C7-1616.

[108] F. Rebillat, J. Lamon, R. Naslain, E. Lara-Curzio, M.K. Ferber, T.M. Besmann, Interfacial bond strength in SiC/C/SiC composite materials, as studied by single-fiber push-out tests, J. Am. Ceram. Soc. 81 (1998) 965–978, https://doi.org/10.1111/j.1151-2916.1998.tb02434.x.

[109] L. Zilong, Y. Jianling, F. Zeyu, H. Xiaozhong, Y. Haitang, Microstructure and mechanical performance of SiC_f/BN/SiC mini-composites oxidized at elevated temperature from ambient temperature to 1500 °C in air, J. Eur. Ceram. Soc. 40 (2020) 2821–2827, https://doi.org/10.1016/j.jeurceramsoc.2019.04.013.

[110] X. Lv, M. Yue, W. Yang, X. Feng, X. Li, Y. Wang, J. Wang, J. Zhang, J. Wang, Tunable strength of SiC_f/β-$Yb_2Si_2O_7$ interface for different requirements in SiC_f/SiC CMC: inspiration from model composite investigation, J. Mater. Sci. Technol. 67 (2021) 165–173, https://doi.org/10.1016/j.jmst.2020.05.071.

[111] S. Bertrand, R. Pailler, J. Lamon, SiC/SiC minicomposites with nanoscale multilayered fibre coatings, Compos. Sci. Technol. 61 (2001) 363–367, https://doi.org/10.1016/S0266-3538(00)00131-7.

[112] R.R. Naslain, R. Pailler, X. Bourrat, S. Bertrand, F. Heurtevent, P. Dupel, F. Lamouroux, Synthesis of highly tailored ceramic matrix composites by pressure-pulsed CVI, Solid State Ionics 141–142 (2001) 541–548, https://doi.org/10.1016/S0167-2738(01)00743-3.

[113] O. Rapaud, S. Jacques, H. Di-Murro, H. Vincent, M.-P. Berthet, J. Bouix, SiC/SiC minicomposites with $(PyC/TiC)_n$ interphases processed by pressure-pulsed reactive CVI, J. Mater. Sci. 39 (2004) 173–180, https://doi.org/10.1023/B:JMSC.0000007742.34926.65.

[114] F.W. Zok, Developments in oxide fiber composites, J. Am. Ceram. Soc. 89 (2006) 3309–3324, https://doi.org/10.1111/j.1551-2916.2006.01342.x.

[115] C. Ben Ramdane, A. Julian-Jankowiak, R. Valle, Y. Renollet, M. Parlier, E. Martin, P. Diss, Microstructure and mechanical behaviour of a Nextel^{TM}610/alumina weak matrix composite subjected to tensile and compressive loadings, J. Eur. Ceram. Soc. 37 (2017) 2919–2932, https://doi.org/10.1016/j.jeurceramsoc.2017.02.042.

[116] D.B. Marshall, R.F. Davis, P.E.D. Morgan, J.R. Porter, Interface materials for damage-tolerant oxide composites, Key Eng. Mater. 127–131 (1996) 27–36. https://doi.org/10.4028/www.scientific.net/KEM.127-131.27.

[117] M. Verdenelli, S. Parola, F. Chassagneux, J.-M. Létoffé, H. Vincent, J.-P. Scharff, J. Bouix, Sol-gel preparation and thermo-mechanical properties of porous xAl_2O_3–$ySiO_2$ coatings on SiC Hi-Nicalon fibres, J. Eur. Ceram. Soc. 23 (2003) 1207–1213, https://doi.org/10.1016/S0955-2219(02)00296-0.

[118] S. Jacques, O. Rapaud, S. Parolla, M. Verdenelli, Which alternative to the pyrocarbon interphase in ceramic matrix composites? Ann. Chim. Sci. Mat. 30 (2005) 609–620, https://doi.org/10.3166/acsm.30.609-620.

[119] I. Jouanny, S. Jacques, P. Weisbecker, C. Labrugère, M. Lahaye, L. Maillé, R. Pailler, Synthesis of TiC from porous carbon coating on Si–C–O (Nicalon) fibres by reactive chemical vapour deposition in pressure-pulsed mode or at atmospheric pressure, J. Mater. Sci. 45 (2010) 6747–6756, https://doi.org/10.1007/s10853-010-4769-9.
[120] S. Jacques, I. Jouanny, O. Ledain, L. Maillé, P. Weisbecker, Nanoscale multilayered and porous carbide interphases prepared by pressure-pulsed reactive chemical vapor deposition for ceramic matrix composites, Appl. Surf. Sci. 275 (2013) 102–109, https://doi.org/10.1016/j.apsusc.2013.01.100.
[121] C.G. Cofer, J. Economy, Oxidative and hydrolytic stability of boron nitride — a new approach to improving the oxidation resistance of carbonaceous structures, Carbon 33 (1995) 389–395, https://doi.org/10.1016/0008-6223(94)00163-T.
[122] N. Kostoglou, K. Polychronopoulou, C. Rebholz, Thermal and chemical stability of hexagonal boron nitride (h-BN) nanoplatelets, Vacuum 112 (2015) 42–45, https://doi.org/10.1016/j.vacuum.2014.11.009.
[123] P. Carminati, S. Jacques, F. Rebillat, Oxidation/corrosion of BN-based coatings as prospective interphases for SiC/SiC composites, J. Eur. Ceram. Soc. 41 (2021) 3120–3131, https://doi.org/10.1016/j.jeurceramsoc.2020.07.056.
[124] V. Cholet, L. Vandenbulcke, J.P. Rouan, P. Baillif, R. Erre, Characterization of boron nitride films deposited from BCl_3-NH_3-H_2 mixtures in chemical vapour infiltration conditions, J. Mater. Sci. 29 (1994) 1417–1435, https://doi.org/10.1007/BF00368905.
[125] P. Carminati, T. Buffeteau, N. Daugey, G. Chollon, F. Rebillat, S. Jacques, Low pressure chemical vapour deposition of BN: relationship between gas phase chemistry and coating microstructure, Thin Solid Films 664 (2018) 106–114, https://doi.org/10.1016/j.tsf.2018.08.020.
[126] M. Chen, L. Pan, X. Xia, W. Zhou, Y. Li, Boron nitride (BN) and BN based multiple-layer interphase for SiC_f/SiC composites: a review, Ceram. Int. (2022), https://doi.org/10.1016/j.ceramint.2022.07.021. S0272884222024087.
[127] H.J. Seifert, F. Aldinger, Phase equilibria in the Si-B-C-N system, in: M. Jansen (Ed.), High Performance Non-oxide Ceramics I, Springer Berlin Heidelberg, Berlin, Heidelberg, 2002, pp. 1–58, https://doi.org/10.1007/3-540-45613-9_1.
[128] R. Haubner, M. Wilhelm, R. Weissenbacher, B. Lux, Boron nitrides — properties, synthesis and applications, in: M. Jansen (Ed.), High Performance Non-oxide Ceramics II, Springer Berlin Heidelberg, Berlin, Heidelberg, 2002, pp. 1–45, https://doi.org/10.1007/3-540-45623-6_1.
[129] C. Schimpf, M.R. Schwarz, C. Lathe, E. Kroke, D. Rafaja, Effect of the microstructure of graphitic boron nitride on the kinetics of the formation of boron nitride high-pressure phases, J. Eur. Ceram. Soc. 39 (2019) 944–951, https://doi.org/10.1016/j.jeurceramsoc.2018.10.021.
[130] M. Chubarov, H. Pedersen, H. Högberg, Z. Czigány, M. Garbrecht, A. Henry, Polytype pure sp^2-BN thin films as dictated by the substrate crystal structure, Chem. Mater. 27 (2015) 1640–1645, https://doi.org/10.1021/cm5043815.
[131] M. Chubarov, H. Högberg, A. Henry, H. Pedersen, Review Article: challenge in determining the crystal structure of epitaxial 0001 oriented sp^2 -BN films, J. Vac. Sci. Technol. A: Vacuum, Surfaces, and Films 36 (2018), 030801, https://doi.org/10.1116/1.5024314.
[132] F.F. Xu, Y. Bando, M. Hasegawa, New phases of sp^2-bonded boron nitride: the 12R and 24R polytypes, Chem. Commun. (2002) 1490–1491, https://doi.org/10.1039/b203144b.
[133] T. Matsuda, N. Uno, H. Nakae, T. Hirai, Synthesis and structure of chemically vapour-deposited boron nitride, J. Mater. Sci. 21 (1986) 649–658, https://doi.org/10.1007/BF01145537.
[134] M.I. Petrescu, M.G. Balint, Structure and properties modifications in boron nitride. Part I: direct polymorphic transformations mechanisms, U.P.B. Sci. Bull., Series B. 69 (2007) 35–42.
[135] T. Takahashi, H. Itoh, M. Kuroda, Structure and properties of CVD-BN thick film prepared on carbon steel substrate, J. Cryst. Growth 53 (1981) 418–422, https://doi.org/10.1016/0022-0248(81)90092-0.
[136] K. Nakamura, Preparation and properties of amorphous boron nitride films by molecular flow chemical vapor deposition, J. Electrochem. Soc. 132 (1985) 1757–1762, https://doi.org/10.1149/1.2114206.
[137] C. Gómez-Aleixandre, A. Essafti, M. Fernández, J.L.G. Fierro, J.M. Albella, Influence of diborane flow rate on the structure and stability of CVD boron nitride films, J. Phys. Chem. 100 (1996) 2148–2153, https://doi.org/10.1021/jp951200d.
[138] N.R. Glavin, C. Muratore, M.L. Jespersen, J. Hu, P.T. Hagerty, A.M. Hilton, A. T. Blake, C.A. Grabowski, M.F. Durstock, M.E. McConney, D.M. Hilgefort, T. S. Fisher, A.A. Voevodin, Amorphous boron nitride: a universal, ultrathin dielectric for 2D nanoelectronics, Adv. Funct. Mater. 26 (2016) 2640–2647, https://doi.org/10.1002/adfm.201505455.
[139] J. Dai, Y. Wang, Z. Xu, R. Mu, L. He, Effect of temperature on the growth of boron nitride interfacial coatings on SiC fibers by chemical vapor infiltration, Ceram. Int. 45 (2019) 18556–18562, https://doi.org/10.1016/j.ceramint.2019.06.077.
[140] V. Cholet, L. Vandenbulcke, Chemical vapor infiltration of boron nitride interphase in ceramic fiber preforms: discussion of some aspects of the fundamentals of the isothermal chemical vapor infiltration process, J. Am. Ceram. Soc. 76 (1993) 2846–2858, https://doi.org/10.1111/j.1151-2916.1993.tb04026.x.
[141] M. Leparoux, L. Vandenbulcke, C. Clinard, Influence of isothermal chemical vapor deposition and chemical vapor infiltration conditions on the deposition kinetics and structure of boron nitride, J. Am. Ceram. Soc. 82 (2004) 1187–1195, https://doi.org/10.1111/j.1151-2916.1999.tb01894.x.
[142] A. Udayakumar, A. Sri Ganesh, S. Raja, M. Balasubramanian, Effect of intermediate heat treatment on mechanical properties of SiC_f/SiC composites with BN interphase prepared by ICVI, J. Eur. Ceram. Soc. 31 (2011) 1145–1153, https://doi.org/10.1016/j.jeurceramsoc.2010.12.018.
[143] H. Plaisantin, S. Jacques, J. Danet, G. Camus, H. Delpouve, TEM characterization of turbostratic and rhombohedral BN interphases synthesized by chemical vapour infiltration in SiC/SiC-Si composites, Mater. Char. 172 (2021), 110857, https://doi.org/10.1016/j.matchar.2020.110857.
[144] R.S. Pease, Crystal structure of boron nitride, Nature 165 (1950) 722–723, https://doi.org/10.1038/165722b0.
[145] H.O. Pierson, Boron nitride composites by chemical vapor deposition, J. Compos. Mater. 9 (1975) 228–240, https://doi.org/10.1177/002199837500900302.
[146] M.Z. Karim, D.C. Cameron, M.S.J. Hashmi, Vapour deposited boron nitride thin films, Mater. Des. 13 (1992) 207–214, https://doi.org/10.1016/0261-3069(92)90026-E.
[147] P.B. Mirkarimi, K.F. McCarty, D.L. Medlin, Review of advances in cubic boron nitride film synthesis, Mater. Sci. Eng. R Rep. 21 (1997) 47–100, https://doi.org/10.1016/S0927-796X(97)00009-0.
[148] M. Becton, X. Wang, Grain-size dependence of mechanical properties in polycrystalline boron-nitride: a computational study, Phys. Chem. Chem. Phys. 17 (2015) 21894–21901, https://doi.org/10.1039/C5CP03460D.
[149] G. Cassabois, P. Valvin, B. Gil, Hexagonal boron nitride is an indirect bandgap semiconductor, Nat. Photonics 10 (2016) 262–266, https://doi.org/10.1038/nphoton.2015.277.
[150] S. Prouhet, G. Camus, C. Labrugere, A. Guette, E. Martin, Mechanical characterization of Si-C(O) fiber/SiC (CVI) matrix composites with a BN-interphase, J. Am. Ceram. Soc. 77 (1994) 649–656, https://doi.org/10.1111/j.1151-2916.1994.tb05344.x.
[151] S. Le Gallet, F. Rebillat, A. Guette, X. Bourrat, F. Doux, Influence of a multilayered matrix on the lifetime of SiC/BN/SiC minicomposites, J. Mater. Sci. 39 (2004) 2089–2097, https://doi.org/10.1023/B:JMSC.0000017771.93067.42.
[152] O. Gavalda-Diaz, R. Manno, A. Melro, G. Allegri, S.R. Hallett, L. Vandeperre, E. Saiz, F. Giuliani, Mode I and Mode II interfacial fracture energy of SiC/BN/SiC CMCs, Acta Mater. 215 (2021), 117125, https://doi.org/10.1016/j.actamat.2021.117125.
[153] G.N. Morscher, H.M. Yun, J.A. DiCarlo, L. Thomas-Ogbuji, Effect of a boron nitride interphase that debonds between the interphase and the matrix in SiC/SiC composites, J. Am. Ceram. Soc. 87 (2004) 104–112, https://doi.org/10.1111/j.1551-2916.2004.00104.x.
[154] F. Rebillat, J. Lamon, A. Guette, The concept of a strong interface applied to SiC/SiC composites with a BN interphase, Acta Mater. 48 (2000) 4609–4618, https://doi.org/10.1016/S1359-6454(00)00247-0.
[155] S. Jacques, A. Lopez-Marure, C. Vincent, H. Vincent, J. Bouix, SiC/SiC minicomposites with structure-graded BN interphases, J. Eur. Ceram. Soc. 20 (2000) 1929, https://doi.org/10.1016/S0955-2219(00)00064-9. –1938.
[156] S. Jacques, B. Bonnetot, M.-P. Berthet, H. Vincent, BN interphase processed by LP-CVD from tris(dimethylamino)borane and characterized using SiC/SiC minicomposites, in: E. Lara-Curzio, M.J. Readey (Eds.), Ceramic Engineering and Science Proceedings, John Wiley & Sons, Inc., Hoboken, NJ, USA, 2004, pp. 123–128, https://doi.org/10.1002/9780470291191.ch20.
[157] R.M.G. De Meyere, L. Gale, S. Harris, I.M. Edmonds, T.J. Marrow, D.E. J. Armstrong, Optimizing the fiber push-out method to evaluate interfacial failure in SiC/BN/SiC ceramic matrix composites, J. Am. Ceram. Soc. 104 (2021) 2741–2752, https://doi.org/10.1111/jace.17673.
[158] H. Delpouve, G. Camus, S. Jouannigot, B. Humez, H. Plaisantin, C. Josse, S. Jacques, Relationship between both thickness and degree of crystallisation of BN interphases and the mechanical behaviour of SiC/SiC composites, J. Mater. Sci. (2022), https://doi.org/10.1007/s10853-022-07753-0.
[159] K. Roder, D. Nestler, D. Wett, B. Mainzer, M. Frieß, L. Wöckel, T. Ebert, G. Wagner, D. Koch, S. Spange, Development of a SiN_x-based barrier coating for SiC fibres, Mater. Sci. Forum 825–826 (2015) 256–263. https://doi.org/10.4028/www.scientific.net/MSF.825-826.256.
[160] B. Mainzer, K. Roder, L. Wöckel, M. Frieß, D. Koch, D. Nestler, D. Wett, H. Podlesak, G. Wagner, T. Ebert, S. Spange, Development of wound $SiC_{BNx/SiNx}$/SiC with near stoichiometric SiC matrix via LSI process, J. Eur. Ceram. Soc. 36 (2016) 1571–1580, https://doi.org/10.1016/j.jeurceramsoc.2015.12.015.
[161] R.T. Bhatt, F. Sola-Lopez, M.C. Halbig, M.H. Jaskowiak, Thermal stability of CVI and MI SiC/SiC composites with Hi-Nicalon^{TM}-S fibers, J. Eur. Ceram. Soc. 42 (2022) 3383–3394, https://doi.org/10.1016/j.jeurceramsoc.2022.03.009.
[162] C.-M. Wang, X. Pan, M. Rühle, F.L. Riley, M. Mitomo, Silicon nitride crystal structure and observations of lattice defects, J. Mater. Sci. 31 (1996) 5281–5298, https://doi.org/10.1007/BF01159294.
[163] W.C. Leslie, K.G. Carroll, R.M. Fisher, Diffraction patterns and crystal structure of Si_3N_4 and Ge_3N_4, J. Occup. Med. 4 (1952) 204–206, https://doi.org/10.1007/BF03397673.
[164] D. Hardie, K.H. Jack, Crystal structures of silicon nitride, Nature 180 (1957) 332–333, https://doi.org/10.1038/180332a0.
[165] B. Vassiliou, F.G. Wilde, A hexagonal form of silicon nitride, Nature 179 (1957) 435–436, https://doi.org/10.1038/179435b0.
[166] A. Zerr, G. Miehe, G. Serghiou, M. Schwarz, E. Kroke, R. Riedel, H. Fueß, P. Kroll, R. Boehler, Synthesis of cubic silicon nitride, Nature 400 (1999) 340–342, https://doi.org/10.1038/22493.
[167] M.T. Duffy, S. Berkman, G.W. Cullen, R.V. D'Aiello, H.I. Moss, Development and evaluation of refractory CVD coatings as contact materials for molten silicon, J. Cryst. Growth 50 (1980) 347–365, https://doi.org/10.1016/0022-0248(80)90259-6.
[168] P. Rocabois, C. Chatillon, C. Bernard, Thermodynamics of the Si-O-N system: I, high-temperature study of the vaporization behavior of silicon nitride by mass

spectrometry, J. Am. Ceram. Soc. 79 (1996) 1351–1360, https://doi.org/10.1111/j.1151-2916.1996.tb08596.x.
[169] H.D. Batha, E.D. Whitney, Kinetics and mechanism of the thermal decomposition of Si_3N_4, J. Am. Ceram. Soc. 56 (1973) 365–369, https://doi.org/10.1111/j.1151-2916.1973.tb12687.x.
[170] A.H. Heuer, V.L.K. Lou, Volatility diagrams for silica, silicon nitride, and silicon carbide and their application to high-temperature decomposition and oxidation, J. Am. Ceram. Soc. 73 (1990) 2789–2803, https://doi.org/10.1111/j.1151-2916.1990.tb06677.x.
[171] N. Jacobson, S. Farmer, A. Moore, H. Sayir, High-temperature oxidation of boron nitride: I, monolithic boron nitride, J. Am. Ceram. Soc. 82 (1999) 393–398, https://doi.org/10.1111/j.1551-2916.1999.tb20075.x.
[172] L.G. Podobeda, A.K. Tsapuk, A.D. Buravov, Oxidation of boron nitride under nonisothermal conditions, Powder Metall. Met. Ceram. 15 (1976) 696–698, https://doi.org/10.1007/BF01157838.
[173] Y. Lei, Y. Wang, Y. Song, Boron nitride by pyrolysis of the melt-processable poly [tris(methylamino)borane]: structure, composition and oxidation resistance, Ceram. Int. 38 (2012) 271–276, https://doi.org/10.1016/j.ceramint.2011.07.001.
[174] S. Willemin, P. Carminati, S. Jacques, J. Roger, F. Rebillat, Identification of complex oxidation/corrosion behaviours of boron nitride under high temperature, Oxid. Metals 88 (2017) 247–256, https://doi.org/10.1007/s11085-017-9739-z.
[175] T. Narushima, T. Goto, Y. Yokoyama, J. Hagiwara, Y. Iguchi, T. Hirai, High-temperature active oxidation and active-to-passive transition of chemically vapor-deposited silicon nitride in N_2-O_2 and Ar-O_2 atmospheres, J. Am. Ceram. Soc. 77 (1994) 2369–2375, https://doi.org/10.1111/j.1151-2916.1994.tb04607.x.
[176] T. Narushima, T. Goto, T. Hirai, Y. Iguchi, High-temperature oxidation of silicon carbide and silicon nitride, Mater. Trans., JIM 38 (1997) 821–835, https://doi.org/10.2320/matertrans1989.38.821.
[177] W.L. Vaughn, H.G. Maahs, Active-to-Passive transition in the oxidation of silicon carbide and silicon nitride in air, J. Am. Ceram. Soc. 73 (1990) 1540–1543, https://doi.org/10.1111/j.1151-2916.1990.tb09793.x.
[178] F. Rebillat, Advances in self-healing ceramic matrix composites, in: Advances in Ceramic Matrix Composites, Elsevier, 2014, pp. 369–409, https://doi.org/10.1533/9780857098825.2.369.
[179] T. Matsuda, Stability to moisture for chemically vapour-deposited boron nitride, J. Mater. Sci. 24 (1989) 2353–2357, https://doi.org/10.1007/BF01174496.
[180] R.M.G. De Meyere, L. Gale, S. Harris, I. Edmonds, A.L. Chamberlain, T.J. Marrow, D.E.J. Armstrong, Micromechanical properties of vapour-exposed SiC_f/BN/SiC ceramic-matrix composites, J. Eur. Ceram. Soc. 42 (2022) 3148–3155, https://doi.org/10.1016/j.jeurceramsoc.2022.02.022.
[181] V.E. Collier, W. Xu, R.M. McMeeking, F.W. Zok, M.R. Begley, Recession of BN coatings in SiC/SiC composites through reaction with water vapor, J. Am. Ceram. Soc. 105 (2022) 498–511, https://doi.org/10.1111/jace.18052.
[182] X. Ma, X. Yin, X. Cao, L. Chen, L. Cheng, L. Zhang, Effect of heat treatment on the mechanical properties of SiC_f/BN/SiC fabricated by CVI, Ceram. Int. 42 (2016) 3652–3658, https://doi.org/10.1016/j.ceramint.2015.11.030.
[183] A. Nöth, J. Maier, K. Schönfeld, H. Klemm, Wet chemical deposition of BN, SiC and Si_3N_4 interphases on SiC fibers, J. Eur. Ceram. Soc. 41 (2021) 2988–2994, https://doi.org/10.1016/j.jeurceramsoc.2020.06.013.
[184] S. Hinke, S. Stöckel, G. Marx, Characterization of BN-films deposited onto carbon fibres by a continuous CVD-process, Fresenius' J. Anal. Chem. 349 (1994) 181, https://doi.org/10.1007/BF00323263, 181.
[185] S. Jacques, H. Vincent, C. Vincent, A. Lopez-Marure, J. Bouix, Multilayered BN coatings processed by a continuous LPCVD treatment onto Hi-Nicalon fibers, J. Solid State Chem. 162 (2001) 358–363, https://doi.org/10.1006/jssc.2001.9387.
[186] M. Suzuki, Y. Tanaka, Y. Inoue, N. Miyamoto, M. Sato, K. Goda, Uniformization of boron nitride coating thickness by continuous chemical vapor deposition process for interphase of SiC/SiC composites, J. Ceram. Soc. Jpn. 111 (2003) 865–871, https://doi.org/10.2109/jcersj.111.865.
[187] S. Stöckel, G. Marx, W.A. Goedel, Coating of ceramic SiC, SiBNC, and Al_2O_3 fibers with SiBN using a continuous CVD process – influence of stoichiometry on stability against oxidation and hydrolysis, Chem. Vap. Depos. 13 (2007) 553–560, https://doi.org/10.1002/cvde.200706626.
[188] Y. Ye, U. Graupner, R. Krüger, Hexagonal boron nitride from a borazine precursor for coating of SiBNC fibers using a continuous atmospheric pressure CVD process, Chem. Vap. Depos. 17 (2011) 221–227, https://doi.org/10.1002/cvde.201106911.
[189] P. Carminati, Composites SiC/SiC à interphase de type BN de compositions variables et réactivité optimisée, PhD, University of Bordeaux, 2016. http://www.theses.fr/2016BORD0248.
[190] J.-S. Park, N. Nakazato, N. Takayama, H. Kishimoto, A. Kohyama, High speed formation of pyro-carbon coat on silicon carbide fiber by continuous chemical vapor deposition furnace, Fusion Eng. Des. 125 (2017) 442–446, https://doi.org/10.1016/j.fusengdes.2017.05.031.
[191] C. Lorrette, P. Weisbecker, S. Jacques, R. Pailler, J.M. Goyhénèche, Deposition and characterization of hex-BN coating on carbon fibres using tris (dimethylamino)borane precursor, J. Eur. Ceram. Soc. 27 (2007) 2737–2743, https://doi.org/10.1016/j.jeurceramsoc.2006.10.010.
[192] M.Q. Brisebourg, F. Rebillat, F. Teyssandier, A new experimental apparatus for in-situ characterization of silica growth during passive corrosion of sic at very high temperatures, Oxid. Metals 80 (2013) 289–298, https://doi.org/10.1007/s11085-013-9386-y.
[193] G. Constant, R. Feurer, Preparation and characterization of thin protective films in silica tubes by thermal decomposition of hexachloroborazine, J. Less Common. Met. 82 (1981) 113–118, https://doi.org/10.1016/0022-5088(81)90206-X.
[194] R.A. Levy, E. Mastromatteo, J.M. Grow, V. Paturi, W.P. Kuo, H.J. Boeglin, R. Shalvoy, Low pressure chemical vapor deposition of B-N-C-H films from triethylamine borane complex, J. Mater. Res. 10 (1995) 320–327, https://doi.org/10.1557/JMR.1995.0320.
[195] C. Rohr, J.-H. Boo, W. Ho, The growth of hexagonal boron nitride thin films on silicon using single source precursor, Thin Solid Films 322 (1998) 9–13, https://doi.org/10.1016/S0040-6090(97)01007-9.
[196] J.-H. Boo, C. Rohr, W. Ho, MOCVD of BN and GaN thin films on silicon: new attempt of GaN growth with BN buffer layer, J. Cryst. Growth 189–190 (1998) 439–444, https://doi.org/10.1016/S0022-0248(98)00323-6.
[197] R.Y. Tay, H. Li, S.H. Tsang, M. Zhu, M. Loeblein, L. Jing, F.N. Leong, E.H.T. Teo, Trimethylamine borane: a new single-source precursor for monolayer h-BN single crystals and h-BCN thin films, Chem. Mater. 28 (2016) 2180–2190, https://doi.org/10.1021/acs.chemmater.6b00114.
[198] K. Nakamura, Preparation and properties of boron nitride films by metal organic chemical vapor deposition, J. Electrochem. Soc. 133 (1986) 1120–1123, https://doi.org/10.1149/1.2108797.
[199] X. Yang, S. Nitta, K. Nagamatsu, S.-Y. Bae, H.-J. Lee, Y. Liu, M. Pristovsek, Y. Honda, H. Amano, Growth of hexagonal boron nitride on sapphire substrate by pulsed-mode metalorganic vapor phase epitaxy, J. Cryst. Growth 482 (2018) 1–8, https://doi.org/10.1016/j.jcrysgro.2017.10.036.
[200] M.D. Allendorf, C.F. Melius, T.H. Osterheld, A model of the gas-phase chemistry of boron nitride CVD from BCl_3 and NH_3, Mater. Res. Soc. Symp. Proc. 410 (1995) 459–464, https://doi.org/10.1557/PROC-410-459.
[201] F.I. Hurwitz, D.R. Wheeler, P.V. Chayka, C. Xu, T.R. McCue, Y.L. Chen, BN and SiBN fiber coatings via CVD using a single source, liquid precursor based on borazine, in: Ceramic Engineering & Science Proceedings, The American Ceramic Society, Cocoa Beach, Florida, 2000, pp. 267–274, https://doi.org/10.1002/9780470294635.ch33.
[202] J.-S. Li, C.-R. Zhang, B. Li, Preparation and characterization of boron nitride coatings on carbon fibers from borazine by chemical vapor deposition, Appl. Surf. Sci. 257 (2011) 7752–7757, https://doi.org/10.1016/j.apsusc.2011.04.024.
[203] N. Sun, C. Wang, L. Jiao, J. Zhang, D. Zhang, Controllable coating of boron nitride on ceramic fibers by CVD at low temperature, Ceram. Int. 43 (2017) 1509–1516, https://doi.org/10.1016/j.ceramint.2016.10.123.
[204] R. Stolle, G. Wahl, Deposition of boron nitride films from BB'B"-trichloroborazine, J. Phys. IV France. 5 (1995) C5–C761, https://doi.org/10.1051/jphyscol:1995590. C5-768.
[205] H. Wu, M. Chen, X. Wei, M. Ge, W. Zhang, Deposition of BN Interphase Coatings from B-Trichloroborazine and its Effects on the Mechanical Properties of SiC/SiC Composites, vol. 257, 2010, pp. 1276–1281, https://doi.org/10.1016/j.Apsusc.2010.08.047, https://doi.org/10.1016/j.apsusc.2010.08.047.
[206] O. Dugne, S. Prouhet, A. Guette, R. Naslain, R. Fourmeaux, Y. Khin, J. Sevely, J. P. Rocher, J. Cotteret, Interface characterization by TEM, AES and SIMS in tough SiC (ex-PCS) fibre-SiC (CVI) matrix composites with a BN interphase, J. Mater. Sci. 28 (1993) 3409–3422, https://doi.org/10.1007/BF01159815.
[207] F. Rebillat, A. Guette, C.R. Brosse, Chemical and mechanical alterations of SiC Nicalon fiber properties during the CVD/CVI process for boron nitride, Acta Mater. 47 (1999) 1685–1696, https://doi.org/10.1016/S1359-6454(99)00032-4.
[208] R. Naslain, R. Pailler, F. Langlais, A. Guette, S. Jacques, X-CVI (with X = I or P), A unique process for the engineering and infiltration of the interphase in SiC-matrix composites: an overview, in: L. Zhang, D. Jiang (Eds.), Ceramic Transactions Series, John Wiley & Sons, Inc., Hoboken, NJ, USA, 2014, pp. 391–401, https://doi.org/10.1002/9781118932995.ch42.
[209] S. Le Gallet, G. Chollon, F. Rebillat, A. Guette, X. Bourrat, R. Naslain, M. Couzi, J. L. Bruneel, Microstructural and microtextural investigations of boron nitride deposited from BCl_3–NH_3–H_2 gas mixtures, J. Eur. Ceram. Soc. 24 (2004) 33–44, https://doi.org/10.1016/S0955-2219(03)00126-2.
[210] Y. Yang, W. Zhang, Chemical vapor deposition of SiC at different molar ratios of hydrogen to methyltrichlorosilane, J. Cent. South Univ. Technol. 16 (2009) 730–737, https://doi.org/10.1007/s11771-009-0121-4.
[211] G. Laduye, CVD du carbure de silicium à partir du système SiH_xC_{4-x}/C_yH_z/H_2 : étude expérimentale et modélisation, University of Bordeaux, 2016. https://tel.archives-ouvertes.fr/tel-01477657.
[212] T.M. Besmann, B.W. Sheldon, M.D. Kaster, Temperature and concentration dependence of SiC deposition on Nicalon fibers, Surf. Coat. Technol. 43–44 (1990) 167–175, https://doi.org/10.1016/0257-8972(90)90071-J.
[213] F. Loumagne, F. Langlais, R. Naslain, S. Schamm, D. Dorignac, J. Sévely, Physicochemical properties of SiC-based ceramics deposited by low pressure chemical vapor deposition from $CH_3SiCl_3H_2$, Thin Solid Films 254 (1995) 75–82, https://doi.org/10.1016/0040-6090(94)06237-F.
[214] Z. Qi, X. Lv, W. Zhao, S. Zhu, J. Jiao, BN/SiC coating on SiC tows prepared by chemical vapor infiltration, IOP Conf. Ser. Mater. Sci. Eng. 678 (2019), 012062, https://doi.org/10.1088/1757-899X/678/1/012062.
[215] K. Petroski, A. Almansour, J. Grady, S.L. Suib, Morphological control of silicon carbide deposited on Hi-Nicalon type S fiber using atmospheric pressure chemical vapor infiltration, ACS Omega 5 (2020) 24811–24817, https://doi.org/10.1021/acsomega.0c03493.
[216] P. Drieux, G. Chollon, S. Jacques, A. Allemand, D. Cavagnat, T. Buffeteau, Experimental study of the chemical vapor deposition from CH_3SiHCl_2/H_2: application to the synthesis of monolithic SiC tubes, Surf. Coat. Technol. 230 (2013) 137–144, https://doi.org/10.1016/j.surfcoat.2013.06.046.

[217] M.-S. Cho, J.-W. Kim, G.-Y. Chung, Manufacturing of ceramic composites reinforced with layered woven fabrics by CVI of SiC from dichlorodimethylsilane, Kor. J. Chem. Eng. 13 (1996) 515–521, https://doi.org/10.1007/BF02706003.
[218] T. Takeuchi, Y. Egashira, T. Osawa, H. Komiyama, A kinetic study of the chemical vapor deposition of silicon carbide from dichlorodimethylsilane precursors, J. Electrochem. Soc. 145 (1998) 1277–1284, https://doi.org/10.1149/1.1838451.
[219] T. Hirai, CVD processing, MRS Bull. 20 (1995) 45–47, https://doi.org/10.1557/S0883769400048946.
[220] Y. Yang, W. Zhang, Kinetic and microstructure of SiC deposited from $SiCl_4$-CH_4-H_2, Chin. J. Chem. Eng. 17 (2009) 419–426, https://doi.org/10.1016/S1004-9541(08)60226-8.
[221] S.-L. Zhang, J.-T. Wang, W. Kaplan, M. Östling, Silicon nitride films deposited from SiH_2Cl_2-NH_3 by low pressure chemical vapor deposition: kinetics, thermodynamics, composition and structure, Thin Solid Films 213 (1992) 182–191, https://doi.org/10.1016/0040-6090(92)90281-F.
[222] A.A. Korkin, J.V. Cole, D. Sengupta, J.B. Adams, On the mechanism of silicon nitride chemical vapor deposition from dichlorosilane and ammonia, J. Electrochem. Soc. 146 (1999) 4203–4212, https://doi.org/10.1149/1.1392615.
[223] M.J. Grieco, F.L. Worthing, B. Schwartz, Silicon nitride thin films from $SiCl_4$ plus NH_3: preparation and properties, J. Electrochem. Soc. 115 (1968) 525, https://doi.org/10.1149/1.2411310.
[224] K. Niihara, T. Hirai, Chemical vapour-deposited silicon nitride: Part 4 Hardness characteristics, J. Mater. Sci. 12 (1977) 1243–1252, https://doi.org/10.1007/BF02426863.
[225] E. Fitzer, D. Hegen, Chemical vapor deposition of silicon carbide and silicon nitride- chemistry's contribution to modern silicon ceramics, Angew. Chem., Int. Ed. Engl. 18 (1979) 295–304, https://doi.org/10.1002/anie.197902951.
[226] S. Motojima, N. Iwamori, T. Hattori, Chemical vapour deposition of Si_3N_4 from a gas mixture of Si_2Cl_6, NH_3 and H_2, J. Mater. Sci. 21 (1986) 3836–3842, https://doi.org/10.1007/BF02431619.
[227] R.C. Taylor, B.A. Scot, LPCVD of silicon nitride films from hexachlorodisilane and ammonia, MRS Proc 105 (1987) 319, https://doi.org/10.1557/PROC-105-319.